2011

MORPHOLOGY, MATERIAL AND VIBRATORY PROPERTIES OF THE SWIMBLADDER IN THE CARP, CYPRINUS CARPIO

Yasha Mohajer
Virginia Commonwealth University

MORPHOLOGY, MATERIAL AND VIBRATORY PROPERTIES OF THE SWIMBLADDER IN THE CARP, *CYPRINUS CARPIO*

A thesis submitted in partial fulfillment of the requirements for the degree of Master of Science at Virginia Commonwealth University

by

YASHA J. MOHAJER
B.S., Virginia Commonwealth University, 2008
M.S., Virginia Commonwealth University, 2011

Director: MICHAEL L. FINE, Ph.D.
Professor, Department of Biology

Virginia Commonwealth University
Richmond, Virginia
August, 2011

Acknowledgement

I would like to first thank Dr. Michael Fine for his assistance and guidance and my committee members: Dr. Jennifer K. Stewart, Dr. Martin L. Lenhardt and Dr. Stephen P. McIninch. I would also like to thank Haris, Aaron, Eun, and Emory for volunteering, my lab mates Zachary, Shweta, Paul, Shelley, Kim and Lettie for the good times, Dr. Karen Kester and Justin for their help, Dave Hopler, Matt Balazik, Ricky Davis and Mindee Coulter for their help and kind donations and the rest of the VCU Biology department. Also, I want to thank my parents, Sarah, Gertie, Elliott, my brother and his wife, and the rest of my family and friends for their endless support.

Table of Contents

List of Figures

Abstract

MORPHOLOGY, MATERIAL AND VIBRATORY PROPERTIES OF THE SWIMBLADDER IN THE CARP, *CYPRINUS CARPIO*

By: Yasha J. Mohajer, M.S.

A thesis submitted in partial fulfillment of the requirements for the degree of Master of Science at Virginia Commonwealth University.

Virginia Commonwealth University, 2011.

Major Director: Michael Fine, Ph.D. Department of Biology

The carp *Cyprinus carpio* has a two-chambered swimbladder and excellent hearing. I explored the hypothesis that the anterior chamber, which connects to Weberian ossicles, is adapted for hearing by testing both chambers for material properties. I also determined displacement and auditory responses to mechanical strikes. Wall stress is higher in the posterior, strain in the anterior and modulus lower in the anterior chamber. Strikes increase pressure followed by a variable rebound that rapidly decays. Displacement and sound amplitude increase with hammer force, and amplitude is similar in both chambers for within chamber strikes but lower across chambers. Normalized for equivalent displacement, the anterior chamber produces a more intense sound. Stiffness and damping are greater for the anterior chamber, but sound spectra are similar. More intense sound production per unit of movement, greater damping and higher stiffness for the anterior chamber should all contribute to high-frequency auditory sensitivity.

Introduction

Teleosts swimbladders function in buoyancy, auditory detection and sound production (Ladich and Fine, 2006). Fish of the superorder Ostariophysi, are able to detect high frequency and low threshold sounds because of a direct connection of the swimbladder to the ears via Weberian ossicles (Braun and Grande, 2008), modified bones of the anterior vertebrae first described by Weber (1820), that provide a pathway to the ears, which enhances sound detection. These fishes, also known as auditory specialists, detect a wider range of frequencies than the auditory generalists, without a direct connection between the swimbladder and the inner ear (Finneran and Hastings, 2000; Yan et al., 2000; Au and Hastings, 2008). Because gas in the swimbladder is subject to Boyle's law, gas volume is dependent upon ambient pressure, which varies directly with water depth. The pressure in the ostariophysan swimbladders is slightly above ambient (Alexander, 1959), which would increase stiffness and increase vibration of the ossicles. Further, withdrawing gas with a syringe results in hearing loss (Anraku et al. unpublished ms).

Evans (1925) described the anatomy of swimbladders of the family Cyprinidae. Cyprinids are otophysans, and the swimbladder is mechanically coupled to the tripus of the Weberian apparatus. There are two chambers (anterior and posterior) connected via a ductus communicans and the posterior chamber is connected to the esophagus through the pneumatic duct. Removal of the anterior swimbladder abolished the saccular response to a dipole sound source vibrating at 50 Hz (Coombs et al. 2010). Yan (personal communication) found that removal of all air from the anterior

chamber of the swimbladder abolished hearing and removal of the posterior chamber still affected hearing, diminishing auditory thresholds by 80%.

Amoser and Ladich (2005) found that carp hearing is only slightly masked in a quiet environment, but when exposed to loud stream and river noises, the hearing threshold increases dramatically. Goldfish *Carassius auratus*, closely related to carp, subjected to noisy conditions exhibited a spike in plasma cortisol, suggesting that enhanced sensitivity may be stressful in certain environments.

Because gas in the swimbladder is subject to Boyle's law, gas volume is dependent upon ambient pressure, which varies directly with water depth. Studies have addressed the importance of swimbladder volume for hearing, where a loss in volume results in hearing loss (Anraku et al. unpublished ms). Under natural conditions, the pressure in the ostariophysan swimbladder is slightly higher than ambient (Alexander 1959).

The role that the swim bladder plays in sound detection and propagation has been controversial (Harris 1964; v. Bergeijk 1964; Barimo and Fine 1998; Fine et al. 2001). Historically, the swimbladder has been modeled as a resonant bubble with a characteristic resonant frequency depending on its size and depth (Harris, 1964). The advantage for sound generation from a resonant structure is that amplification of sound would require little energy (Michelsen, 1978). The underwater bubble model predicts that sound will emanate from a single source and be distributed equally in all directions (omnidirectional) with an elastic propagated pressure wave. Amplitude would decrease as a function of $1/r^2$ away from the center of the sphere (Bergeijk, 1964).

The resonant bubble model does not explain how the fundamental frequency of the toadfish, *Opsanus tau*, changes seasonally or that a chorus of toadfish of different sizes can have similar fundamental frequencies (Fine, 1978). Further, the toadfish produces a directional sound field that

mirrors the shape of the swimbladder (Barimo and Fine, 1998). Additionally, the walls of the swimbladder are responsible for damping and providing a low Q value (Fine, 1983; Fine *et al.* 2001).

Rapid damping of the toadfish swimbladder appears to relate to its high water content and anisotropic structure with collagen fibers oriented in longitudinal and circular directions (King, 2005). Sound production from the swimbladder of the oyster toadfish excited by stimulation of the sonic nerve (Fine et al. 2001) or with a piezoelectric hammer (Fine *et al.*, 2009) damps more rapidly than predicted for an underwater bubble. These studies determined that sound is produced as a forced response and not a resonant property of the swimbladder. Note there are differences in sound (sharpness of tuning or Q and damping but not peak frequency) produced in air and water (Fine et al. 2004), but the basic findings still hold.

As hypothesized by Evans (1925) the anterior chamber of the carp swimbladder, a non-vocal cyprinid, may be adapted for hearing. The purpose of this study is to investigate the properties of the anterior and posterior chambers of the swimbladder of the carp (*Cyprinus carpio*). I therefore tested whether the two chambers exhibit differences in morphology, tested the material of both chambers on a material test machine and acoustical properties when excited by a piezoelectric hammer. Regressions of responses to hammer amplitude in Newtons allow a comparison of vibration and sound generation of both chambers to comparable stimuli.

Materials and Methods

Eight fish were acquired from the aquaculture station in Virginia State University and categorized by size as small (four fish ranging 26 to 32 cm) or large (four fish ranging 40 to 50 cm). The fish were euthanized with 300 mg MS-222/L in aerated water and measured for total length (TL), weight, swimbladder length (SL). The fish were clamped upside down in a specially modified tank. An incision was made from the anus to the chin, the abdominal muscles were separated, and organs moved aside to expose the ventral side of the swimbladder.

A Doppler-shift laser vibrometer (Brül & Kjaer model 3544; sensitivity 1 V/mm) was aligned to a retro-reflective disc placed on the ventral swimbladder to measure displacement (Fig. 1). An Etymotics ER-7C probe tube microphone (+20 dB amplification) was positioned 1 cm above the disc. Sound amplitude was calibrated with a 1 kHz, 94 dB re: 20 μPa (dB SPL) test tone through a port in the microphone power supply. The swimbladder was stimulated with a miniature model analysis hammer (PCB model 086D80; X10 setting; with a vinyl tip cover, transducer sensitivity 13.91 mV/N).

The anterior (A) and posterior (P) bladders (within chambers) were struck with a series of hits of increasing amplitude. Displacement and sound were recorded at the retro-reflective disc. Both the strike target and the disc were placed on the ventral midline of the bladder (Fig. 1). Across chamber recordings made with strikes against the anterior bladder recorded from the posterior chamber (AP) and vice versa (PA) (Fig. 1).

All analog data were captured, digitized (20 kHz sampling rate) and analyzed with a data acquisition/analysis system (Biopac systems Inc. MP150 Workstation version 3.7). Frequency spectra were determined with a Fast Fourier Transform (FFT, Hamming window 300 ms resolution) for hammer force, swimbladder displacement and sound. Amplitude and duration were determined for each half cycle of the sound, displacement and hammer force traces for each fish.

The damping ratio zeta, ζ was calculated from successive cycles of decay modified to compare the amplitude decay of half cycles (first positive,

P1, and second negative, N2, wave amplitude):

$$\zeta = \ln\left(P1/N2\right) \Big/ \sqrt{\pi^2 + \left[\ln\left(P1/N2\right)\right]^2}$$

The sharpness of tuning (Q) is measured from the zeta value:

$$Q = 1/2(\zeta)$$

And Q was also calculated from the sound spectra, of the small, medium and larger fish:

$$Q = f_{\max}/\Delta f_{-3dB}$$

where f_{max} is the dominant frequency and Δf_{-3dB} is the bandwidth of the "half-power points" on either side of f_{max} whose amplitudes are 3dB lower than the amplitude at f_{max}.

Material properties of swimbladder tissue were determined on an EnduraTEC Bose Electroforce (ELF) 3200 Test Machine. The swimbladder was placed on a cutting board and cut laterally to separate the dorsal and ventral sides. The ventral section was then flattened against the board, and 0.9% NaCl was applied to keep the swimbladder moist. A dogbone-shaped stamp was used to cut a tissue sample from the anterior or posterior swimbladder. The dogbone was oriented parallel to the longitudinal or perpendicular to the longitudinal axis of the swimbladder. A longitudinal and circular sample was taken from both chambers.

The dogbone sample was placed on the flat surface of a microscope slide adjacent to the edge, and the thickness and width of the thinnest region were measured with a stereo microscope and digital camera. The sample was then clamped in the test machine. The bottom clamp was adjusted so the tissue sample was taut but not stretched. The distance between the clamps (gauge length) was measured in millimeters, and the sample was pulled to failure with a maximal excursion of 6.150 mm.

Data were analyzed for stress (force acting on a material divided by the area), strain (relative change in length, $\Delta l/l$), and Young's Modulus (stiffness, measured by stress over strain) and toughness (area under the stress-strain curve) of the sample. Young's Modulus was measured as the slope of the linear regression of the steepest region of the stress-strain curve.

Results

Morphology

The carp swimbladder is separated into anterior and posterior chambers (Fig. 1), connected by a small ductus communicans, not visible externally. Therefore, erroneously, both chambers appear to be separate units externally. Both chambers are held in place by various peritoneal membranes, which also attach the dorsal surface of the swimbladder to the ventral surface of the vertebral column. The anterior chamber is larger in size, wider and less rounded than the posterior chamber, which tapers posteriorly. The anterior chamber has a heavy white collagenous tunica externa with three major layers. The internal and middle layers contain fibers with circular orientation and fibers of the outer layer with longitudinal orientation. The anterior edge of the outer white layer tends to separate from the bladder during dissection, perhaps because of attachments to the Weberian ossicles (Fig. 2).

The posterior chamber is more translucent, thinner, tapering to a point in the caudal end, and held less rigidly, perhaps because of its rounder shape. A gentle push can slightly displace the bladder in the dorsal and lateral direction. Therefore the posterior chamber provides a smaller and less stable target than the anterior chamber for hammer strikes. The posterior chamber wall is composed of two layers of tissue with circular fibers on the outer surface and longitudinal fibers inside. Two dark red bands originate from the anterior end and extend longitudinally from the lateral-ventral surface to the posterior end (Fig. 3). Both the fibers and red bands spiral as they extend to the posterior end of the chamber (Fig. 4). Additionally, the

anterior end of the inner wall of the posterior chamber has about 15 – 25 (varying due to bifurcation) shallow longitudinal stays of varying heights (0.5 – 2 mm in a 56 cm fish) that extend posteriorly for as much as 30% of the chamber length, although only some of them extend this far. Some stays bifurcated at their anterior ends. Stays occur around the sides and dorsal but not ventral surfaces and appear to resist bending of the swimbladder. Some stays terminate in fibers in the bladder that coil as they extend toward the caudal end (Fig. 5), which we interpret as an adaptation to resist lateral movement.

The pneumatic duct is immediately ventral of the ductus communicans so that there are two openings on the forward ventral wall of the posterior chamber (Fig. 6). The pneumatic duct forms a long thick tube that attaches to the ventral surface of the anterior chamber and then terminates through a wide opening in the esophagus (Fig. 7).

Material Properties

Thickness of the anterior chamber wall was 1.3 ± 0.3 (S.E.) mm, which is thicker than the posterior chamber (0.6 ± 0.1 mm; $T_8 = 2.619$, $p = 0.0307$) (Fig. 8).

Peak load was slightly lower for the anterior than the posterior chamber wall ($F_{3,16} = 2.715$, $p = 0.0899$) (Fig. 10). There was no significant difference in toughness between circular and longitudinal pulls for the anterior and posterior chambers ($F_{3,16} = 2.219$, $p = 0.1255$), but posterior circular pulls had the highest toughness with mean 1.0 ± 0.1MPa.

Peak stress was higher for posterior circular pulls (1.3 ± 0.3 MPa) and 0.9 ± 0.2 MPa for longitudinal ones (Fig. 11). Anterior circular sections (0.14 ± 0.03 MPa) had a lower peak stress than both posterior sections ($F_{3,33} = 10.42$, $p < 0.0001$) and anterior longitudinal sections (0.3 ± 0.1MPa) were lower than posterior circular sections (Fig. 11).

Strain at failure was higher for anterior circular sections (1.0 ± 0.1) than posterior circular (0.05 ± 0.1) and posterior longitudinal (0.4 ± 0.1) ($F_{3,36}$ =4.884, p = 0.006). Strain for anterior longitudinal sections (0.8 ± 0.1) was between anterior circular and posterior sections but the difference did not reach significance (Fig. 11).

Young's Modulus, calculated from the slope of the stress strain graph (Fig. 9), was higher in the posterior chamber ($F_{3,29}$ = 24.17, p < 0.0001) with 6.2 ± 0.9 MPa for circular sections and 4.2 ± 0.9 MPa for longitudinal sections. Young's Modulus for the anterior chamber was 0.22 ± 0.05 MPa for circular sections and 0.4 ± 0.2 MPa for longitudinal sections (Fig. 11).

Hammer Strikes

The waveform of hammer force exhibited a single, positive, slightly-asymmetrical half cycle with a shorter rise than fall time (Fig. 12). The rise time represents energy transfer from the hammer to the swimbladder, and the fall time represents the hammer rebound from the swimbladder surface. As hammer force returned to baseline, the force sometimes dropped slightly below baseline but promptly returned (Fig. 12).

Displacement of the anterior swimbladder occurred over 1 – 2.5 cycles and began with a positive half cycle (P1) 1.5 – 2.5 ms after onset of the hammer strike (see latency below) because pressure increased inside the chamber, therefore pushing the swimbladder surface outward toward the laser sensor. The peak of displacement occurred just after peak force from the strike indicating that internal pressure was still pushing the bladder outward. Rebound of the swimbladder caused a negative, asymmetrical half cycle (N1) with reduced amplitude and frequency. The inflection point between P1 and N1 exhibited a slight discontinuity near the end of hammer contact (Fig. 12 arrows). Variable low amplitude, higher frequency waves made N1 difficult to categorize.

The sound waveform consisted of 1 – 2.5 cycles and began with a negative peak of acoustic pressure (N1) caused by bladder compression (not visible on the displacement waveform), followed by a lower frequency positive peak (P1). Hammer force peaked at the end of the first sound cycle. A second lower amplitude cycle followed (N2 and P2). The sound damped quickly and ended approximately a quarter cycle after hammer duration. At times, a sharp, high amplitude negative peak was produced at P2 just following the end of the hammer strike (Fig. 2, posterior). This peak was associated with hammer force dropping below baseline and might have been caused by the bladder briefly adhering to the hammer. The sound waveform was similar between anterior and posterior chambers in larger fish but in smaller fish, the posterior chamber tended to have a greater number of high frequency cycles which may have been caused by the chamber's smaller size. Also, the looser attachment and tendency for movement of the whole chamber may have interfered with the rebounding force on the swimbladder, augmenting hammer duration. The loss of this difference in larger fish may be a result of a larger and strongly adhered swimbladder requiring more energy to displace.

Quantitative Effects of Increasing Hammer Force

Duration

Hammer

All regressions come from 1 large individual fish, which is generally representative of all fish but may not be. Hammer duration was relatively constant with a mean of 16.1 ± 0.5 ms for the anterior chamber (five of eight fish) although it decreased (slope significantly different from zero) in three fish. Variation was similar for the posterior chamber (18.1 ± 0.5 ms; no change in 4, a decrease in 3 and an increase in 1). However, a plot of all fish (Fig. 14) indicates that weaker hits below 0.25 N were longer ranging between 20.5 – 40 ms before stabilizing around

23 ms between 0.25 and 0.5 N. Duration was more variable for the posterior chamber. Duration adjusted for a 0.63 N strike was longer for the posterior than the anterior chamber ($t_{14} = 3.161$, $p = 0.0069$), respectively 18.2 ± 0.6 ms and 23.5±1.6 ms (Fig. 15).

Displacement

P1 and N1 (Fig. 16a) (18.8 ± 2.1 ms and 51.1 ± 15.2, respectively) did not generally vary with hammer force (six fish, although N1 was considerably longer and more variable, P1 and N2 in one fish and decreased in another). Duration of the first cycle (P1 + N1) with mean of 80.2 ± 15.4 ms generally did not generally vary (five fish, decrease in one and increase in two). Total duration at 401.9 ± 66.94 again did not vary in five of eight fish (Fig. 16c). Overall, hammer force did not affect duration for anterior chamber strikes. Similarly duration of P, AP and PA displacements (Fig. 17-19) did not generally vary with hammer force. It is not clear why some fish had significant changes in duration with hammer force, but they were in the minority.

Within chamber displacements were similar for A and P strikes (Fig. 20 a – d). Within chamber responses (A and P) for N1, first cycle and total displacement were longer than cross chamber responses (AP and PA). Total displacement duration was longer for P than AP and PA ($F_{3,28} = 5.346$, $p = 0.005$) .

Sound

P1 and N1 sound duration (3.0 ± 0.3 ms and 5.0 ± 0.4 ms respectively, Fig. 16d and e) did not vary with hammer force in five of eight fish, although N1 decreased in 1 and P1 increased in 2 individuals. The first cycle (N1 + P1), averaging 8.0 ± 0.6 ms, decreased in one fish but did not change in the other seven (Fig. 16e). Total sound duration (Fig. 16f) at 25.5 ± 1.3 ms, increased in two fish but did not vary in the other six. Overall, hammer force did not clearly affect sound duration of the anterior swimbladder.

Sound duration was similar for different strikes with a few exceptions. In the posterior chamber (Fig. 17), total sound duration increased with hammer force in five of eight fish (however with an insignificant decrease in the representative fish). Total sound duration also increased for AP strikes (Fig. 18, representative fish not significant), however, displacement and sound duration did not vary for PA strikes (Fig. 19).

Anterior strikes 0.5 – 1 ms longer than posterior strikes, but differences were not significant. For reasons that are unclear, N1 sound for A was longer than the cross chamber response PA ($F_{3,25} = 3.456$, $p = 0.03$) (Fig. 20e). No other differences were found between responses within or across chambers.

Displacement Latency

Displacement latency for A, (2.0 ± 0.2 ms) did not vary in six of eight fish (Fig. 21). Similar results were found for different hammer strikes in individual fish (P, AP and PA). P strikes below 0.25 N were longer than for harder strikes ranging 1.5 – 9.0 ms before stabilizing at 22 ms between 0.25 and 0.5N (one outlier included in plot with strong hits but long latency, Fig. 21b). Adjusted values for the latency of a 0.5 N strike were calculated (excluding the outlier) to compare within and across chambers (Fig. 22). For the large fish, within chamber latencies (2.4 ± 0.3 ms for A and 1.9 ± 0.3 ms for P) were shorter than for across chambers, which were approximately twice as long (4.6 ± 0.61 ms for AP and 4.0 ± 0.11 ms for PA) (Fig. 22b). Similar results were present for all fish (Fig. 22a), but significance was not as clear. Larger swimbladders may have accentuated the difference.

Displacement Amplitude

For the anterior chamber, P1 ranging from 312 – 905 μm, increased in six fish but did not vary in two and N1, from 184 – 310 μm increased in 7 but did not change in another (Fig.

23a). The amplitude of the first cycle, ranging from 525 – 1216 μm increased in seven and did not change in two (Fig. 23b). Amplitude of P, AP and PA displacements also increased with hammer force with only two exceptions (Fig. 24 – 26). N1 amplitude for P and AP increased in four fish, but did not change in another four. P1 and N1 amplitude of P was greater than AP and PA (Fig. 27 a and b). The amplitudes of the first cycle of A and P were greater than AP and PA (Fig. 27c).

Sound Amplitude

N1 ranged from 82 – 225 mV equivalent 97 – 105 dB SPL, P1 from 92 – 250 mV equivalent 96 – 106 dB SPL and the first cycle, from 175 – 476 mV equivalent 103 – 112 dB SPL, increased in all fish for the anterior chamber (Fig. 23 c and d). Under this regime of hammer strikes, the dynamic range was about 10 dB. Amplitudes for P, AP and PA also increased with hammer force (Fig. 24 – 26). For linear sound N1 amplitude for A was higher than the cross chamber responses AP and PA ($F_{3,25} = 6.878$, $p = 0.01$) and higher in P than for AP, but when measured in decibels, within chamber responses A and P were higher than across chambers AP and PA ($F_{3,25} = 9.891$, $p = 0.0002$) (Fig. 27 d and g). P1 ($F_{3,25} = 13.71$, $p = 0.002$; $F_{3,25} = 18.60$, $p < 0.0001$) and first cycle amplitudes ($F_{3,25} = 10.10$, $p = 0.006$; $F_{3,25} = 15.27$, $p < 0.0001$) for within chamber responses A and P are greater than across for AP and PA for sound measured in both mV and decibels (Fig. 27 e, f, h and i).

Effects of P1 Displacement on Evoked Sound Amplitude

Evoked sound amplitude N1 increased from 82 – 226 mV (96 – 105 dB SPL), P1 increased from 93 – 251 mV (97 – 106 dBV) and N1+P1 increased from 175 – 476 mV (103 – 112 dB SPL) for the anterior chamber with P1 displacement in seven of eight fish (Fig. 28). The posterior chamber yielded in similar findings (Fig. 29). For AP, N1, P1 and the first cycle of

evoked sound did not vary for five fish, but increased in three (Fig. 30). For PA, N1 did not vary with four fish but increased in one, P1 increased in four and did not change in another, and N1+P1 increased in three but did not change in two (Fig. 31). Slopes for N1 ($T_9 = 2.499$, $p = 0.03$), P1 ($T_9 = 2.602$, $p = 0.03$) and the first cycle ($T_9 = 2.729$, $p = 0.02$) were higher for A than P (Fig. 32).

Structural Stiffness

Stiffness did not increase with hammer force for the anterior or posterior chambers, (1.40 ± 0.15 and 1.65 ± 0.17 N/mm) (Fig. 33). For the adjusted value of a 0.63 N hit, structural stiffness was greater in A than P ($T_{14} = 2.044$, $p = 0.03$) with the respective means 1.74 ± 0.37 and 0.88 ± 0.56 (Fig. 34).

Zeta

For A, the coefficient of damping (zeta) averaged 0.10 ± 0.01 and did not vary with hammer force in six fish, increased in one and decreased in another. Findings were similar for P, AP and PA (Fig. 35). Zeta was significantly higher ($T_7 = 2.549$, $p = 0.0381$) for A than P (0.06 ± 0.03) (Fig. 36).

Sharpness of tuning, Q

Sharpness of tuning, Q3dB, was 0.52 ± 0.07 for A and 0.48 ± 0.10 (Fig. 37). There was no significant difference between the two chambers ($T_7 = 0.8979$, $p = 0.3991$).

Frequency Response

Spectral analyses (FFTs) were performed for a representative carp for hammer strikes of varying amplitudes (0.45, 0.83 and 1.32 N), displacement and sound (Fig. 38). For hammer strikes, peak frequency did not vary with increasing hammer force; however stronger hits had

energy at higher frequencies. Stronger hits had greater harmonic waves at 60 Hz intervals, which were reflected in displacement and sound traces.

Peak frequency of displacement and sound did not vary notably with hammer force. Harder hits had greater energy at high frequencies. Also there are more harmonic waves in stronger hits, which take longer to drop back to baseline. The sound spectrograph was relatively flat to 350 Hz indicating that sound energy extended to higher frequencies than the displacement measured at the target disc.

Discussion

Acoustically, the swimbladder has been described as a pulsating resonant underwater bubble, an omnidirectional (monopole) source for sound production and hearing (Harris 1964; Bergeijk 1964). However the swimbladder wall is a highly damped structure and does not exhibit a clear resonant peak (Fine 1983; Barimo and Fine 1998; Fine et al. 2001). Sound detection is aided by the Weberian pathway from the swimbladder to the ears in ostariophysan fishes including the carp (Braun and Grande, 2008; Finneran and Hastings, 2000). Evans (1925) hypothesized that the anterior chamber of the swimbladder was adapted for audition, and the posterior chamber for buoyancy. To help elucidate swimbladder contributions to the Weberian pathway in carp, I investigated the anatomy, material properties and mechanical properties of the anterior and posterior chambers of the swimbladder wall. Previous work on material properties of the carp swimbladder was integrated into this study (King 2005).

Anatomy

The anterior swimbladder is comprised of 3 major layers of tissue. The outer layer contains longitudinal fibers while the middle and inner layers have circular fibers. The anterior chamber adheres to the vertebral column via peritoneal membranes, and a network of mesentery supports the bladder within in the abdominal cavity. Additionally, the tripus, the first bone in the Weberian apparatus attaches to the dorsal-anterior wall, likely providing some degree of support. Finally, the anterior chamber is compressed by the posterior swimbladder, which butts tightly against it. Yan (personal communication) found removal of gas volume from the anterior chamber would diminish

the carp hearing ability, and removal of the posterior chamber increased auditory thresholds by 80%. It is unclear if any of this loss is caused by deflation of the anterior chamber as removal of the posterior chamber will cut through the ductus communicans. The posterior swimbladder may compress the anterior swimbladder to some degree, thereby increasing hoop stress.

Material Properties

The posterior chamber has a lower strain and higher stress and therefore a higher Young's modulus than the anterior chamber. The Young's modulus of the carp posterior chamber is higher than the swimbladder wall of toadfish, catfish and tilapia (values range 0.15 to 1.3 MPa) (Nawaz, 2005 and King, 2005). It also requires a somewhat higher load at failure ($p = 0.09$). The stays and the spiraling of fibers in the chamber appear to allow the bladder to bend considerably during large tail movements without crimping. The anterior chamber has higher percent water (84.5 ± 0.7) than the posterior chamber (78 ± 0.7) (King, 2005). This extra fluid may be used to serve as a lubricant between the 3 different tissues, and may allow the tissue layers to slide past each other, which contributes to the greater strain at break for the anterior chamber. The loosely suspended caudal tip may offer an advantage for hearing by reflecting shearing forces from vibration toward the anterior chamber. The greater strain and lower modulus of the anterior chamber suggests that it would vibrate with a greater amplitude than the posterior chamber in a sound field and likely reflects an adaptation that would amplify movement of the Weberian ossicles.

Acoustic Properties

Striking the swimbladder forces the wall inwards, increasing chamber pressure. Increased pressure from the strike results in the outward movement of the wall at the target disk, initiating displacement P1. The delay between the hammer force and displacement reflects the time necessary to build pressure inside the chamber. N1 displacement begins immediately after the hammer strike.

The 1.5 – 2.5 cycles of displacement are determined by gas pressure inside the bladder and the elastic property of the swimbaldder wall. After termination of the hammer strike (the forced component) near the inflection point between P1 and N1, the displacement waveform (Fig. 11). Half cycles continually increase in duration but decrease in amplitude indicating a damped, non-resonant response and suggesting a complex interaction of gas pressure and wall properties.

Most of the sound occurs during P1 displacement and hammer contact, after which, sound quickly damps. Therefore sound is a result of the forced response of the hammer against the bladder wall. Sound is highly damped beginning with sharp negative pressure N1, following a sharp positive pressure, P1. N1 and P1 may be the result of the initial contact between the hammer tip and chamber wall, occurring before peak of hammer force. N2 and P2, with much weaker amplitudes, proceed after the peak of hammer force and near peak P1 displacement.

Effects of hammer force

Strike duration was generally independent of hammer force except for weak strikes (< 0.25 N) in the posterior chamber. Weak strikes will require more time to build pressure in the chamber. Hammer strikes against the posterior chamber are longer than the anterior chamber and may result, at least partially, from the hammer displacing the loosely held posterior chamber against the abdominal cavity as well as from hammer force that compresses the chamber.

Increasing hammer force against the swimbladders of toadfish, catfish and tilapia resulted in a decrease in duration of displacement and the first cycle of sound, but an increase in total sound (Fine, 2009 and Nawaz, 2005). Hammer force did not affect displacement or sound duration in carp except for total sound duration which increased for the posterior chamber and across chambers for AP.

Displacement and sound amplitude increased with hammer force. For within chamber strikes, evoked sound amplitude increased with displacement. For across chamber strikes, displacement in the anterior chamber resulted in a greater increase in evoked sound than the same displacement for the posterior. This result may be due to a larger surface area capable of emitting a louder sound, but may also be a result of greater stiffness of the posterior chamber, which would transfer more energy to the anterior chamber.

Goldfish (*Carrasius arturus*) have a hearing bandwidth between around 50 Hz to 1.5 kHz with greatest sensitivity between 400 – 1000 Hz (Popper and Schilt, 2008). We stimulated the swimbladder with a relatively low frequency (less than 100 Hz). However, under the same conditions, evoked sound was louder in carp (between 95 – 115 dB) than the oyster toadfish (between 65 – 80 dB) (Fine 2009). This demonstrates that the swimbladder of a non-vocal fish is preadapted for sound production.

Stiffness

The anterior chamber was stiffer than the posterior chamber, with an adjusted mean of 1.73 N/mm and 0.88 N/mm respectively for a 0.63N hit. Therefore as the anterior bladder is being displaced, the energy used to displace the bladder will result in a stronger rebound and higher amplitude of vibration. Stiffness in the anterior bladder may therefore contribute to greater sound amplitude and may be an adaptation to transmission of high frequency reception of ostariophysians. These results are different than those of tilapia and catfish. In tilapia with a single chambered swimbladder, strikes measured between the anterior and posterior sections of the chamber were 0.17 N/mm and 7.6 N/mm respectively (Nawaz, 2005). The catfish had a similar value for stiffness of 1.4 N/mm for anterior-lateral strikes, but the anterior central was far stiffer at 47.6 N/mm because of damping by the transverse septa.

Bladder tuning and Damping

The damping coefficients (zeta) of displacement for the anterior and posterior chambers were 0.1 and 0.75 respectively; support for the chamber wall to be a highly damped structure. Damping is important for the anterior chamber because of coupling to the tripus. A resonant structure would compromise acoustic function by continuing to vibrate after sound termination. Both chambers have lower zeta coefficients than toadfish (0.33), catfish or tilapia (both 0.37) and are just below the range of automobile shock absorbers (0.1 – 0.5) (Steidel, 1989).

Literature Cited

Alexander, R. McN. (1959). The physical properties of the swim bladder in intact Cypriniformes. *J.Exp.Biol.* 36, 315-332

Amoser, S. and Ladich, F. (2010). Year-round variability of ambient noise in temperature freshwater habitats and its implications for fishes. *Aquat. Sci.* 72, 371-378.

Au, W. W. L. and Hastings, M. C. (2008). Hearing in Marine Animals. In: *Principles of Marine Bioacoustics* (eds. Beyer, R. T. and Hartmann, W.), pp. 337-400.Springer Sci.

Barimo, J. F. and Fine, M. L. (1998). Relationship of swim-bladder shape to the directionality pattern of underwater sound in the oyster toadfish. *Can.J.Zool.* 76, 134-143.

Bergeijk, W. A. v. (1964). Directional and nondirectional hearing in fish. In: *Marine bio-acoustics* (ed. Tavolga, W. N.), pp. 281-299. New York: Pergamon Press.

Braun, C. B. and Grande T. (2008). Evolution of Peripheral Mechanisms for the Enhancement of Sound Reception. In: *Fish Bioacoustics* (eds. Webb J. F., Popper A. N., Fay R. R.), pp. 99-144.Springer Sci.

Coombs, S., Fay, R. R., and Elepfandt, A. (2010) Dipole source encoding and tracking by the goldfish auditory system. *J.Exp.Biol.* 213, 3536-3547

Evans, H. M. (1925) A contribution to the anatomy and physiology of the air-bladder and Weberian ossicles in Cyprinidae. *Proceedings of the royal society of London*. 97, 545-576.

Fine, M. L., King, C. B., and Cameron, T. M. (2009). Acoustical properties of the swimbladder in the oyster toadfish *Opsanus tau*. *J.Exp.Biol.* 212. 3542-3552

Fine, M. L. (1978). Seasonal and geographic variation of the mating call of the oyster toadfish *Opsanus tau. Oecologia* 36, 45-57.

Fine, M. L. (1983). Frequency response of the swimbladder of the oyster toadfish. *Comp.Biochem.Physiol.* 74A, 659-663.

Fine, M. L. *et al.* (2001). Movement and sound generation by the toadfish swimbladder. *J.Comp.Physiol.* 187A, 371-379.

Fine, M. L., Schrinel, J. and Cameron, T. M. (2004). The effect of loading on disturbance sounds of the Atlantic croaker *Micropogonious undulatus*: air *vs* water. *J. Acoust. Soc. Amer.* 116, 1271-1275

Finneran, J. J., and Hastings, M. C. (2000). A mathematical analysis of the peripheral auditory system mechanics in the goldfish (*Carassius auratus*). *J. Acoust. Soc. Am*. 108, 1308-1321.

Harris.G.G. (1964). Considerations on the physics of sound production by fishes. In: *Marine bio-acoustics* (ed. Tavolga, W. N.), pp. 233-247. New York: Pergamon Press.

King, T. L. The Relationship Between Collagen Fibers and Material Properties of Swim Bladders in Sonic Teleosts. 2005. M.S. Thesis, Virginia Commonwealth University.

Ladich, F. (1999). Did Auditory Sensitivity and Vocalization Evolve Independently in Otophysan Fishes? *Brain Behav.Evol.* 53, 288-304.

Ladich, F. and Fine, M. L. (2006). Sound-generating mechanisms in fishes: a unique diversity in vertebrates. In: Communication in Fishes. (ed. F. Ladich, S. P. Colin, P. Moller and B. G. Kapoor), pp. 3-43. Enfield, New Hampshire: Science Publishers.

Michelsen, A. (1978). Sound Reception in Different Environments. In: *Sensory Ecology: Review and Perspectives* (ed. Ali, M. A.), pp. 345-373.Springer.

Nawaz, M. A. Material and Acoustic Properties of Swimbladders of Tilapia and Channel Catfish. 2005. M.S. Thesis, Virginia Commonwealth University.

Popper, A. N. and Schilt, C. R. (2008). Hearing and Acoustic Behavior. In: *Fish Bioacoustics* (eds. Webb J. F., Popper A. N., Fay R. R.), pp. 17-48. Spring Sci.

Steidel, R. F. (1989). An Introduction to Mechanical Vibration. New York: Wiley.

Tavolga, W. N. (1964). Sonic characteristics and mechanisms in marine fishes. In: *Marine bio-acoustics* (ed. Tavolga, W. N.), pp. 195-211. New York: Pergamon Press.

Weber E. H. (1820). De Aure et Auditu Hominis et Animalium. Pars I. De Aure Animalium Aquatilium. Leipzig: Gerhard Fleischer.

Yan H. Y., Fine M. L., Horn, N. S., and Colon, W. E. (2000). Variability in the role of the gasbladder in fish audition. *J.Comp.Physiol.* 187A, 371-379.

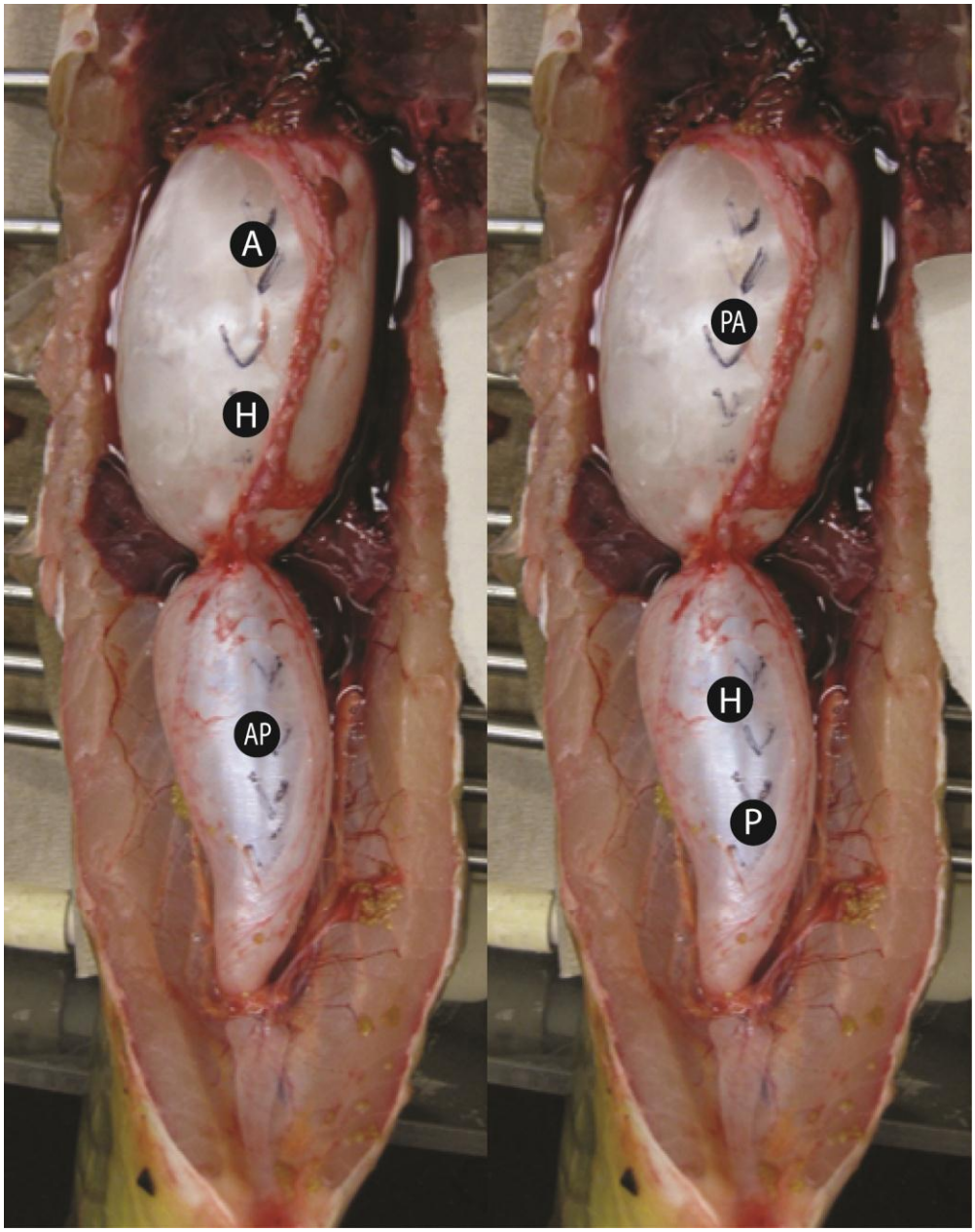

Figure 1: Ventral view of the carp swimbladder showing anterior (top) and posterior chambers (bottom). H indicates strike targets for within and across chamber strikes, A and P indicate site of target disc strikes, and AP indicates disc for strikes of the anterior chamber and PA the posterior chamber for across chamber strikes.

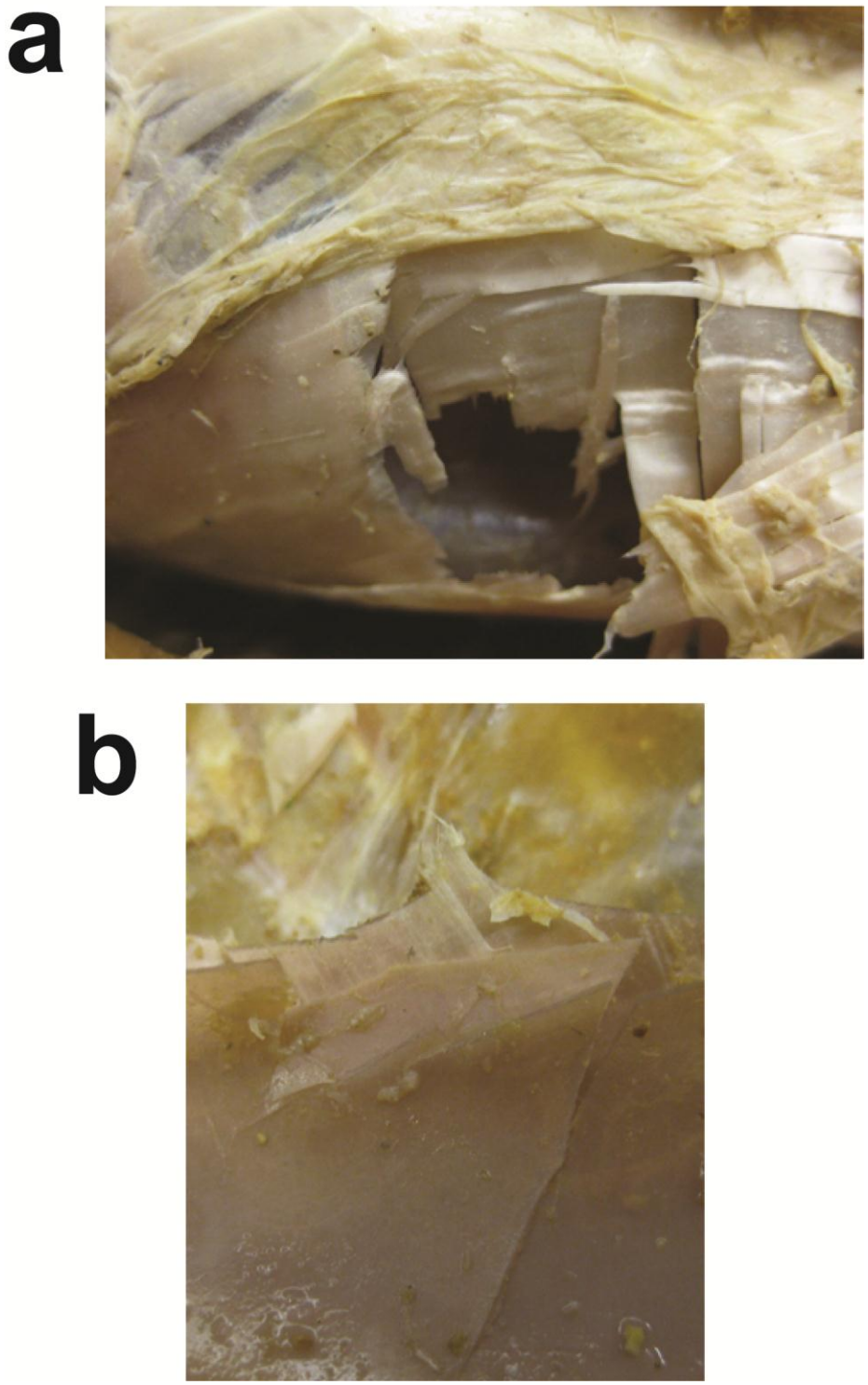

Figure 2: Anterior swimbladder. (a) The anterior swimbladder is composed of different layers with fibers oriented in different directions. (b) Sections of anterior swimbladder (three major layers visible) connected to dorsal wall.

Figure 3: Photograph of ventral view of the posterior chamber. Anterior is to the right; note red band from the side curving over ventral surface, suggesting a spiral although circular bands of collagen are visible.

Figure 4: Anterior view of the lumen of the posterior chamber. Note spiraling of circular fibers.

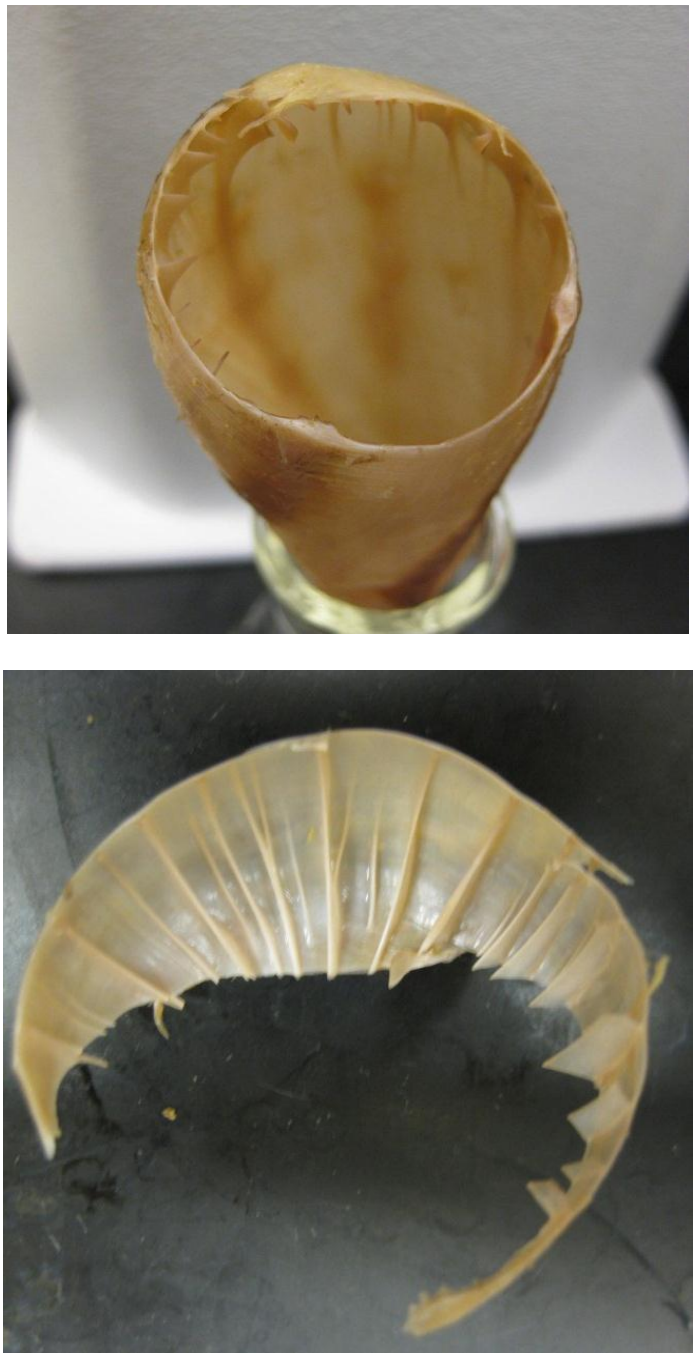

Figure 5: Excised anterior lip of posterior chamber illustrating stays around the sides and dorsal surface (bottom). Stays continue for a short distance in posterior chambers (top).

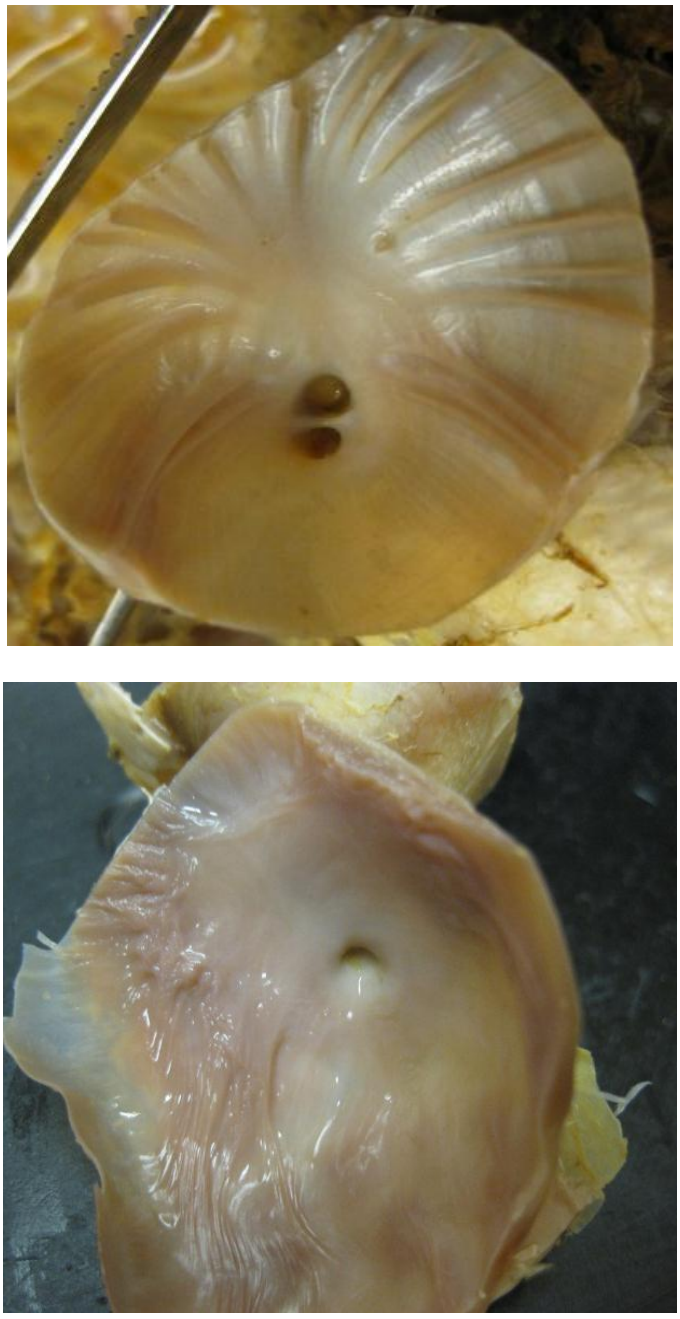

Figure 6: Inner wall of posterior chamber illustrating ductus communicans (right hole) and the pneumatic duct (left hole) (top). Inner wall of anterior chamber showing ductus communicans (bottom).

Figure 7: Connection of anterior and posterior chambers via the ductus connunicans near ventral surface (top, the posterior chamber was tipped upward). The pneumatic duct extends over ventral surface of the anterior chamber. The pneumatic duct and its opening to the esophagus.

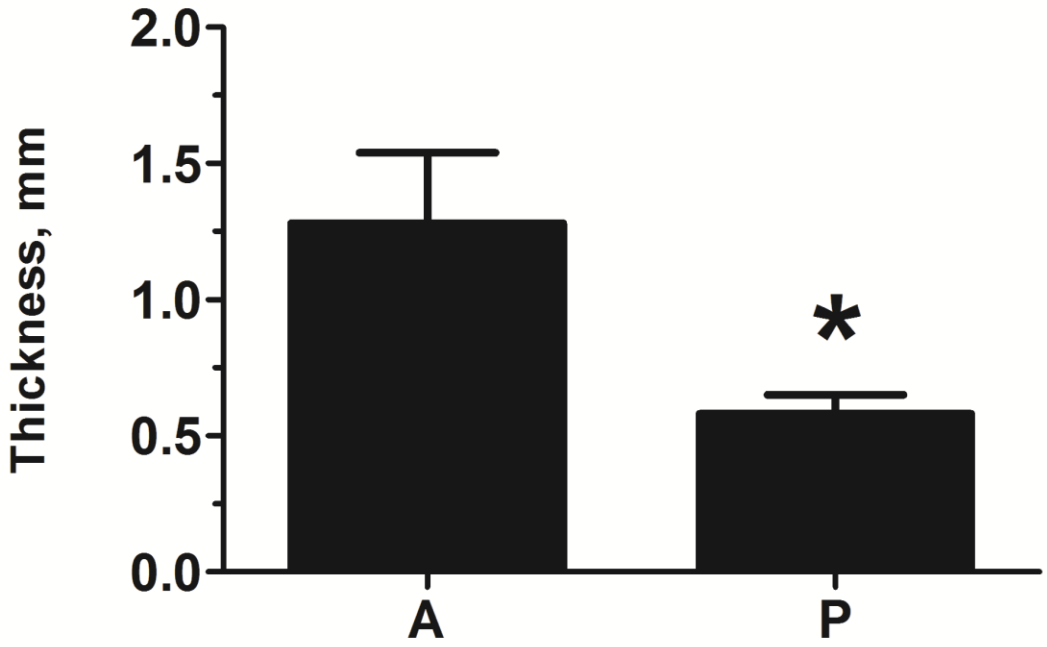

Figure 8: Wall thickness of the anterior (1.3 ± 0.3 mm) (A) and posterior (0.6 ± 0.1 mm) (P) chambers. ($T_8 = 2.619$, $p = 0.0307$)

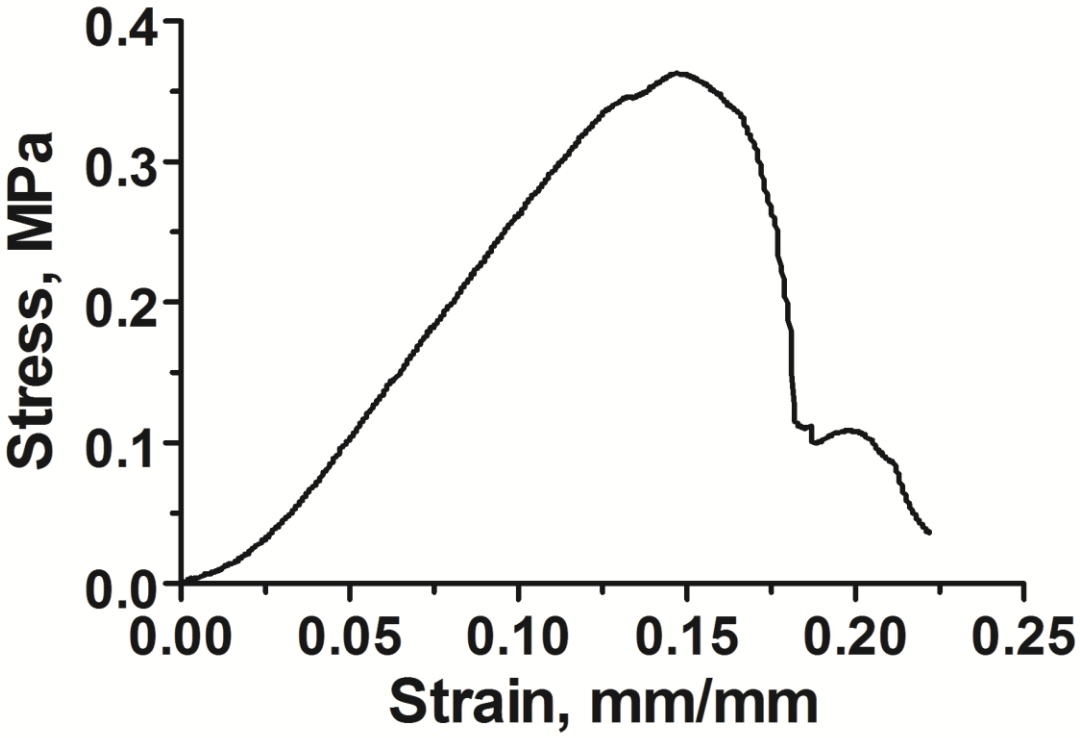

Figure 9: Stress vs. strain graph of material property testing of swimbladder wall.

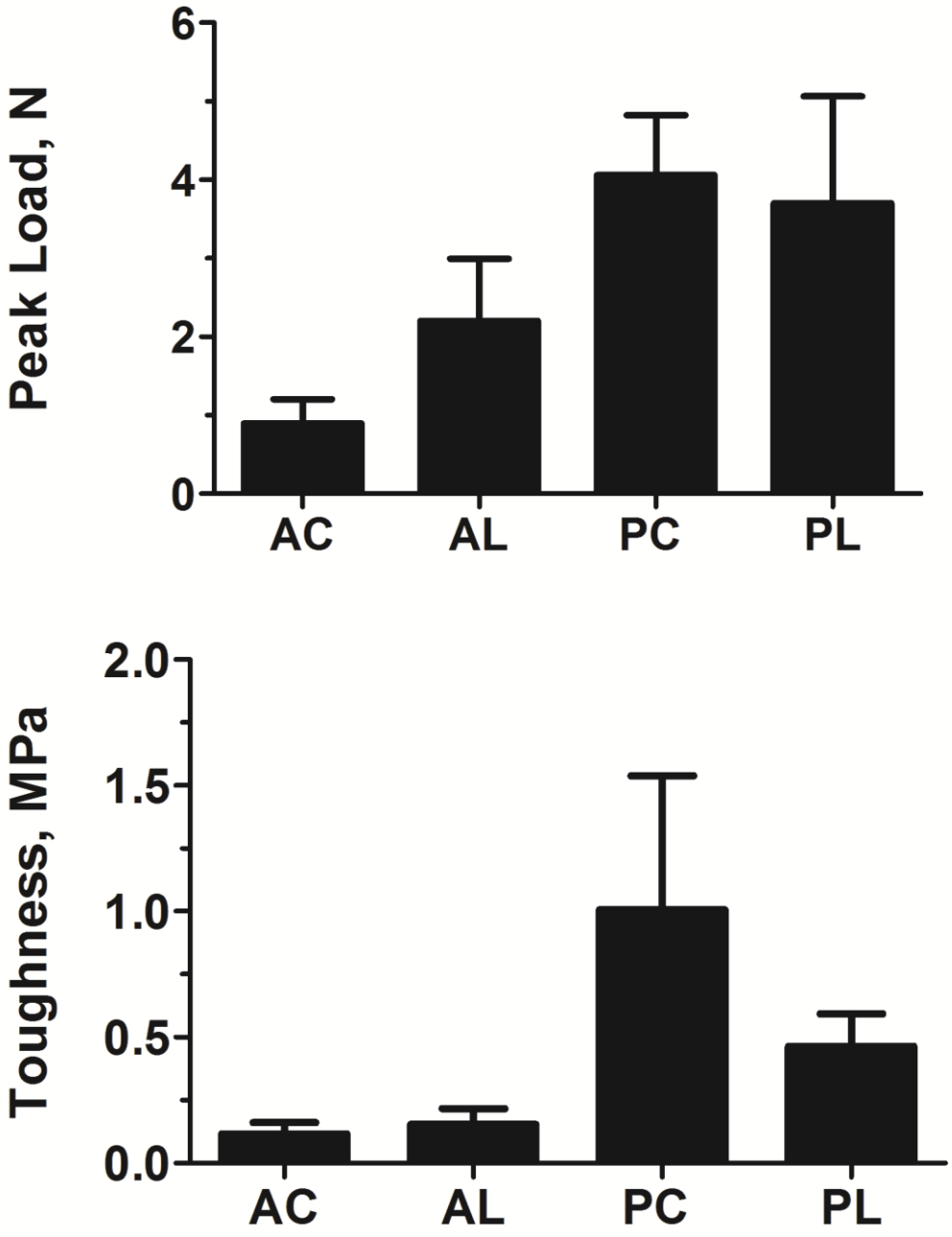

Figure 10: Peak load ($F_{3,16}$ = 2.715, p = 0.0899) and toughness ($F_{3,16}$ = 2.219, p = 0.1255) for the circular (AC) and longitudinal (AL) sections from the anterior and posterior (PC and PL) chamber wall. Peak load and toughness for AC = 0.9 ± 0.3, 0.12 ± 0.04, AL = 2.2 ± 0.8, 0.15 ± 0.06, PC = 4.1 ± 0.8, 1.0 ± 0.5 and PL = 3.7 ± 1.4, 0.5 ± 0.1.

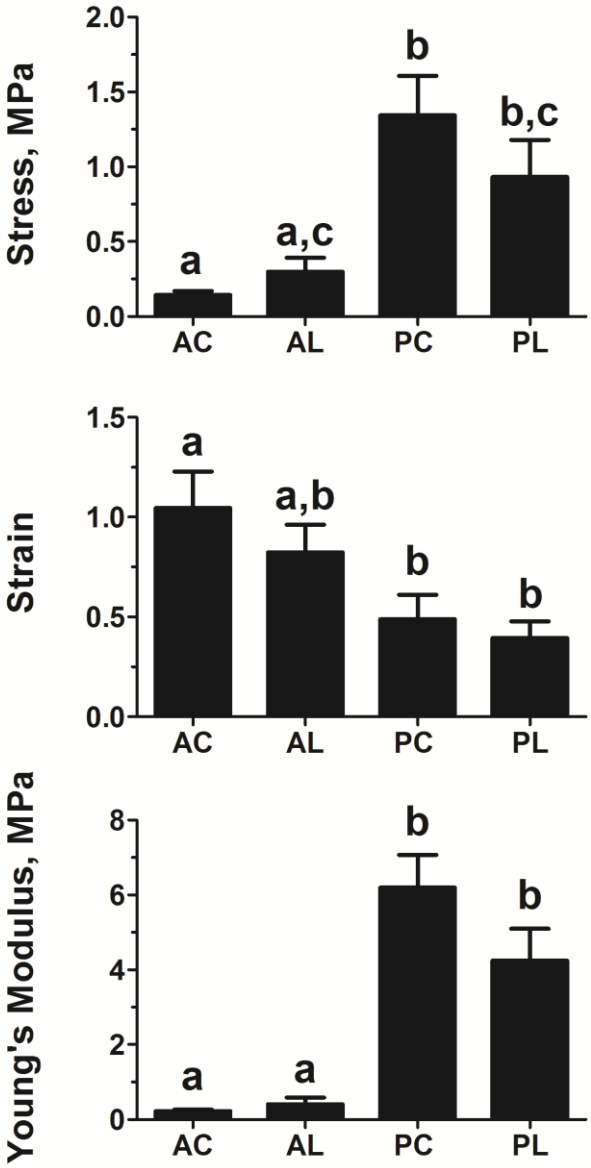

Figure 11: Stress ($F_{3,33}$ = 10.42, $p < 0.0001$), strain ($F_{3,36}$ =4.884, $p = 0.006$) and Young's Modulus ($F_{3,29}$ = 24.17, $p < 0.0001$) for circular (AC) and longitudinal (AL) sections from the anterior and posterior (PC and PL) chamber wall. Stress, Strain and Young's Modulus for AC = 0.14 ± 0.03, 1.0 ± 0.2, 0.22 ± 0.05, AL = 0.30 ± 0.09, 0.8 ± 0.1, 0.4 ± 0.2, PC = 1.3 ± 0.3, 0.5 ± 0.1, 6.2 ± 0.9, PL = 0.9 ± 0.2, 0.39 ± 0.8, 4.2 ± 0.9.

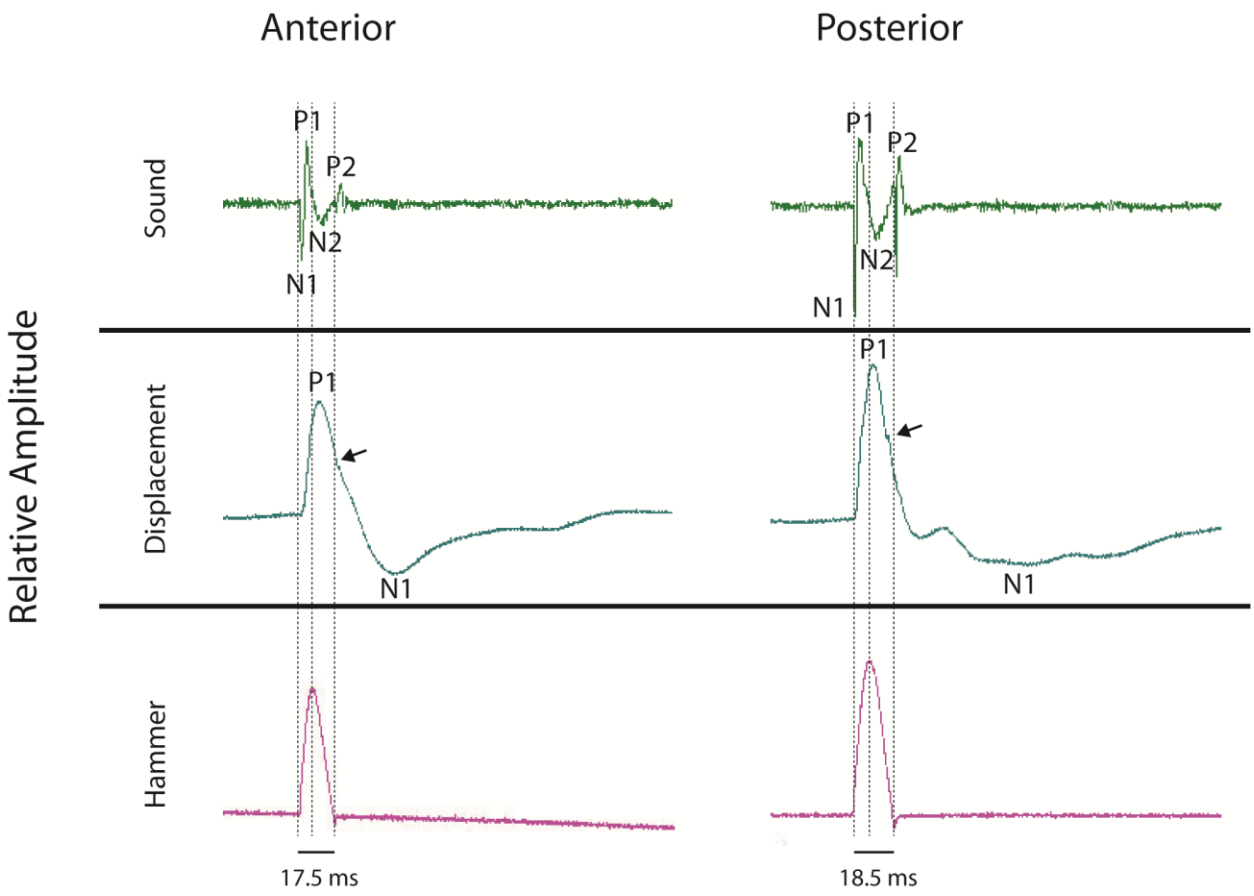

Figure 12: Within chamber waveform of hammer force (bottom), swimbladder displacement (middle) and sound (top) evoked by striking the anterior and posterior swimbladder of a carp. Amplitudes of anterior and posterior waveforms are the same scale. Cursors mark the beginning, peak and end of the hammer strike in a carp representative of 8 fish.

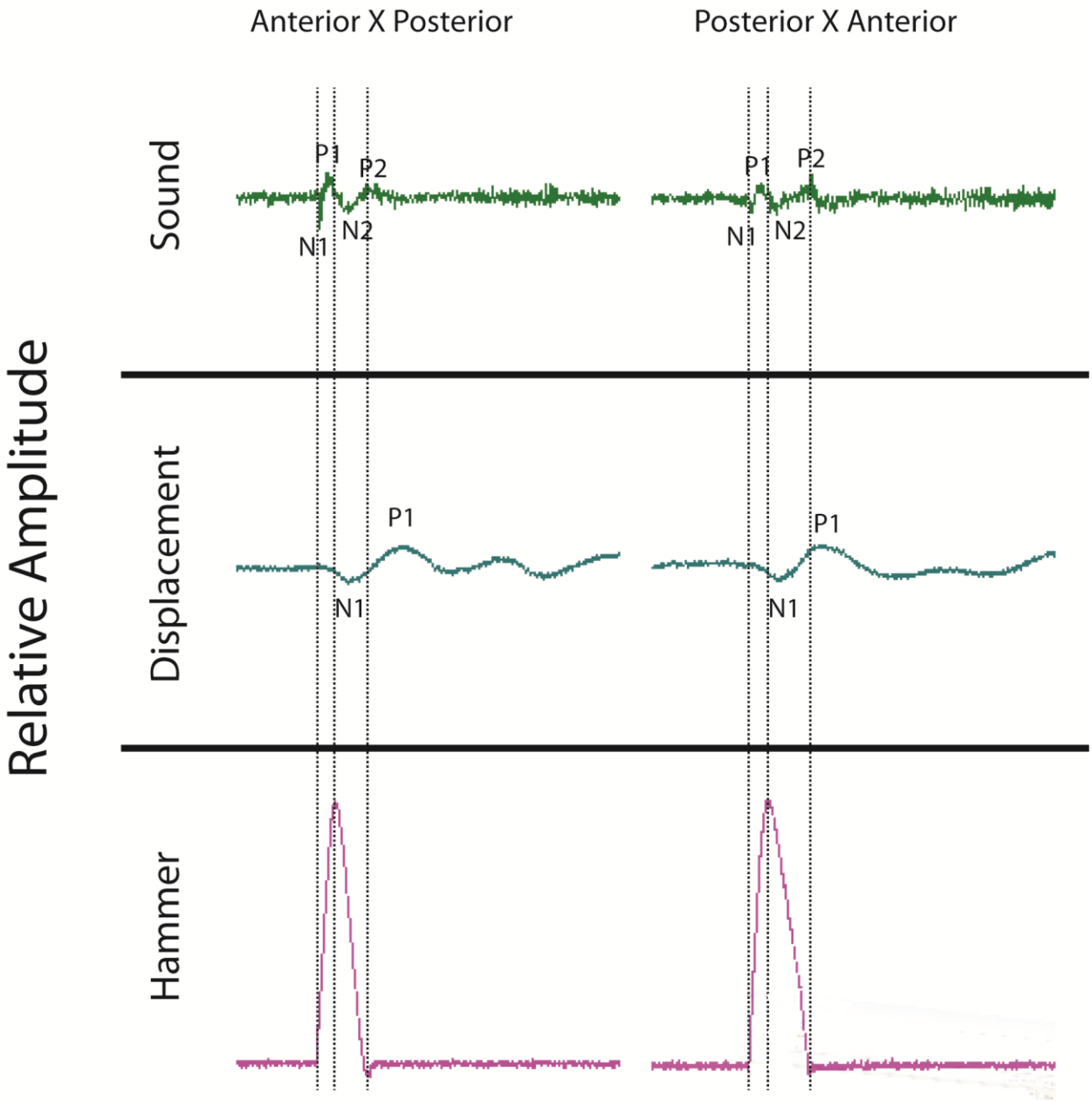

Figure 13: Waveform of hammer force (bottom), swimbladder displacement (middle) and sound (top) evoked by striking the anterior chamber and measuring the posterior response (Left) and striking the posterior chamber and measuring the anterior response (Right). Cursors mark the beginning, peak and end of the hammer strike in a carp representative of 8 fish.

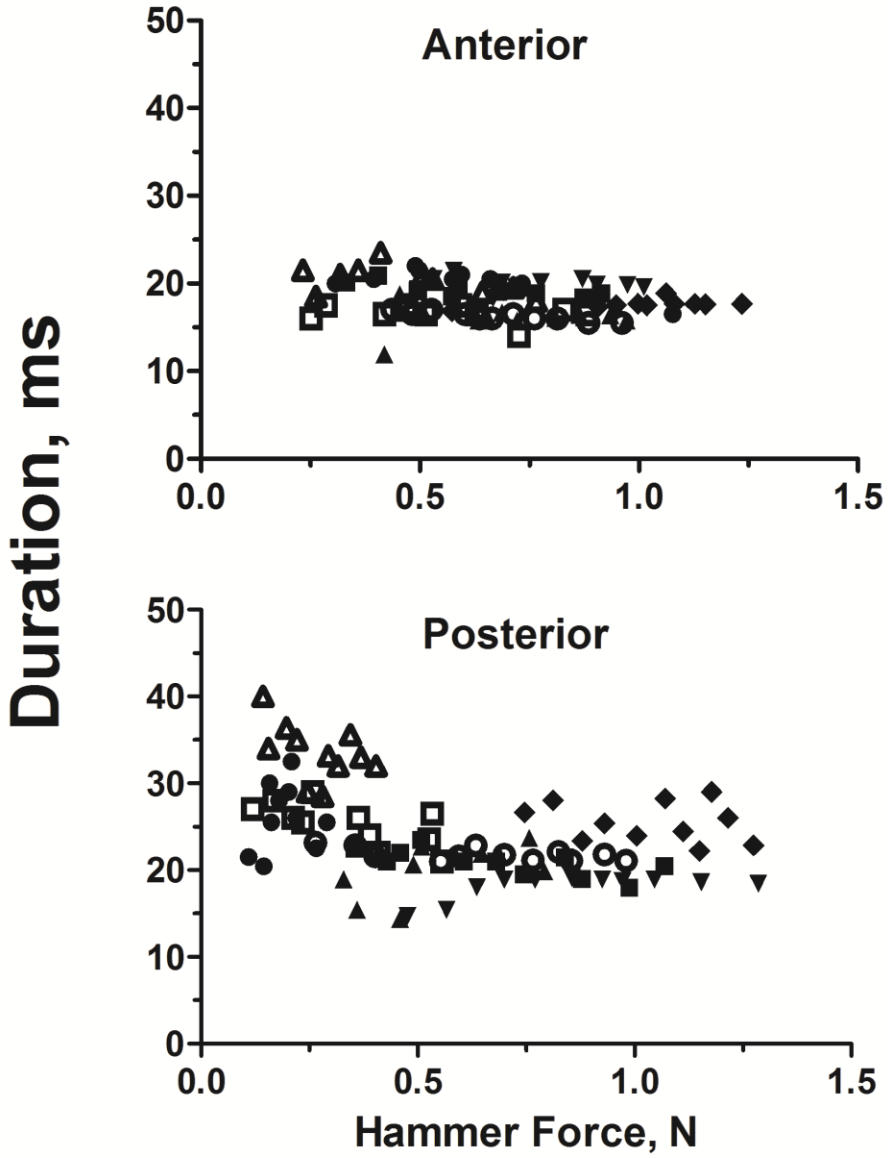

Figure 14: Relationship of hammer force (N) against contact duration (ms) for the anterior and posterior chambers. Different symbols represent individual fish.

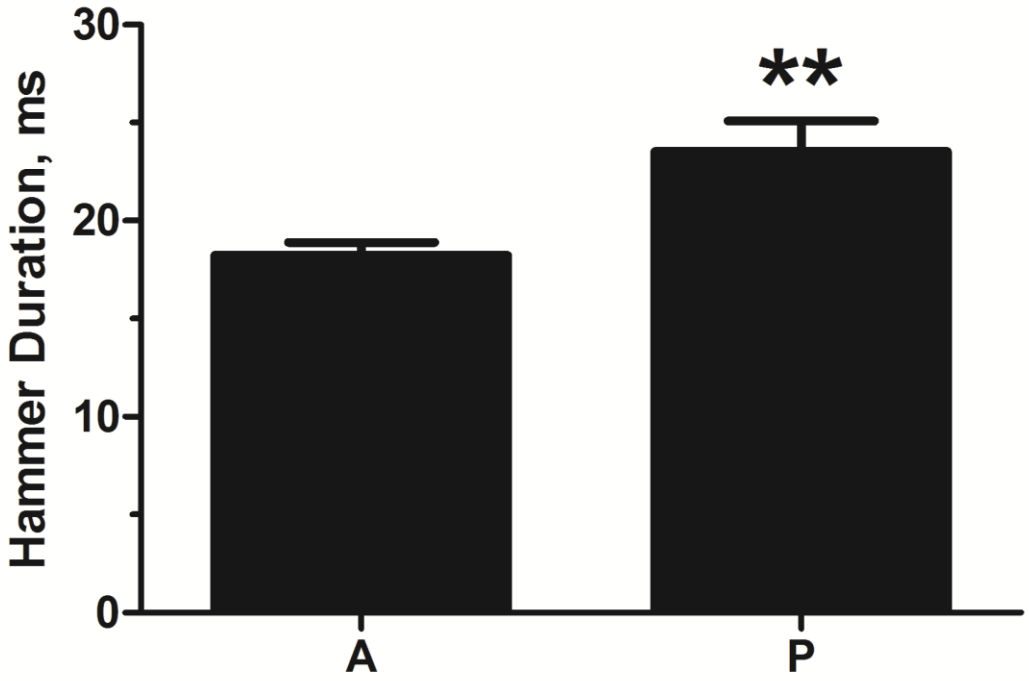

Figure 15: Duration of contact between hammer and swimbladder wall during hammer strikes of anterior (18.2 ± 0.6) and posterior (23.5 ± 1.6) chambers (t_{14} = 3.161, p = 0.0069).

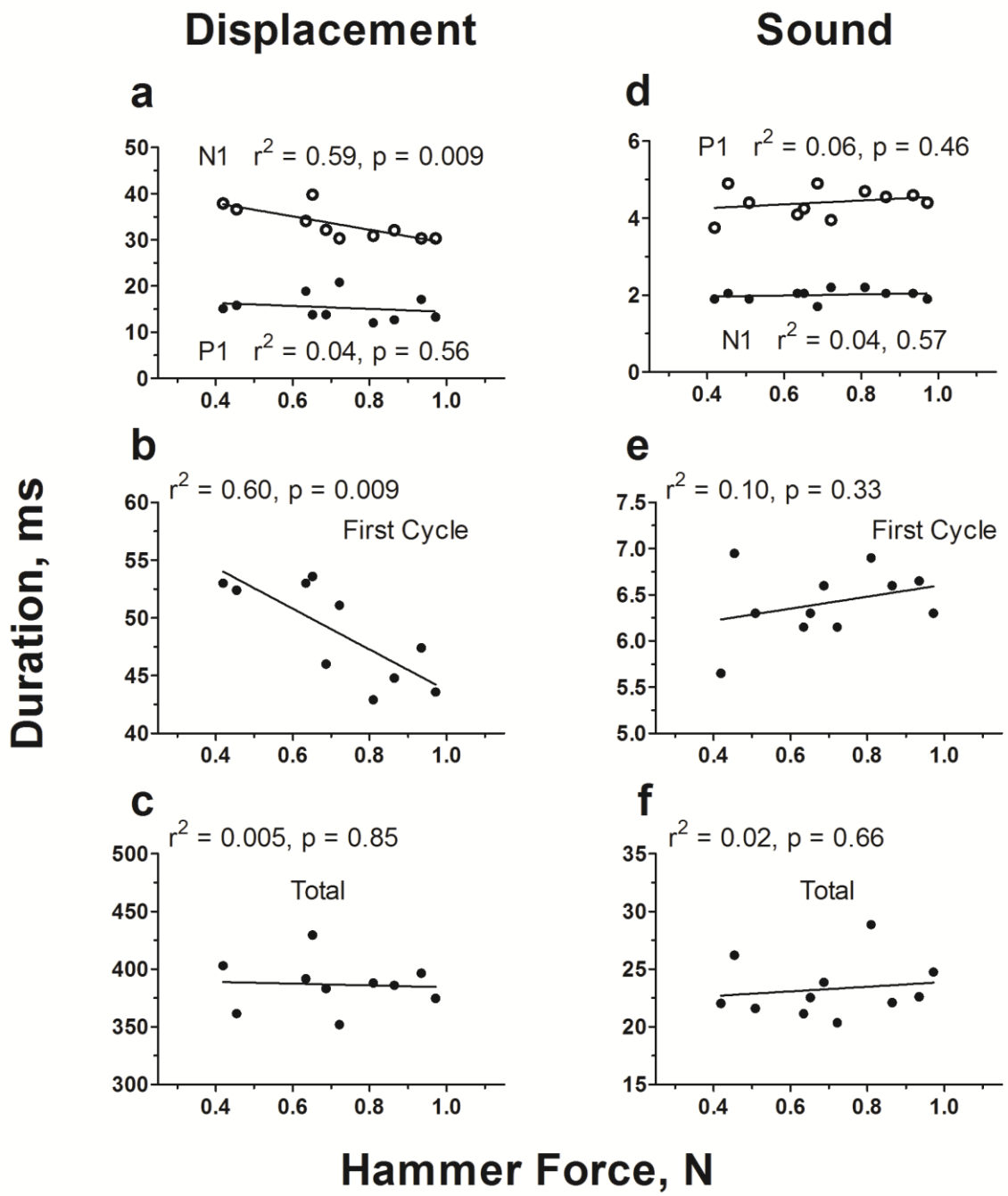

Figure 16: Relationship of displacement and sound (N1, P1, First Cycle, Total) duration to hammer force for the anterior chamber of a carp representative of 8 fish.

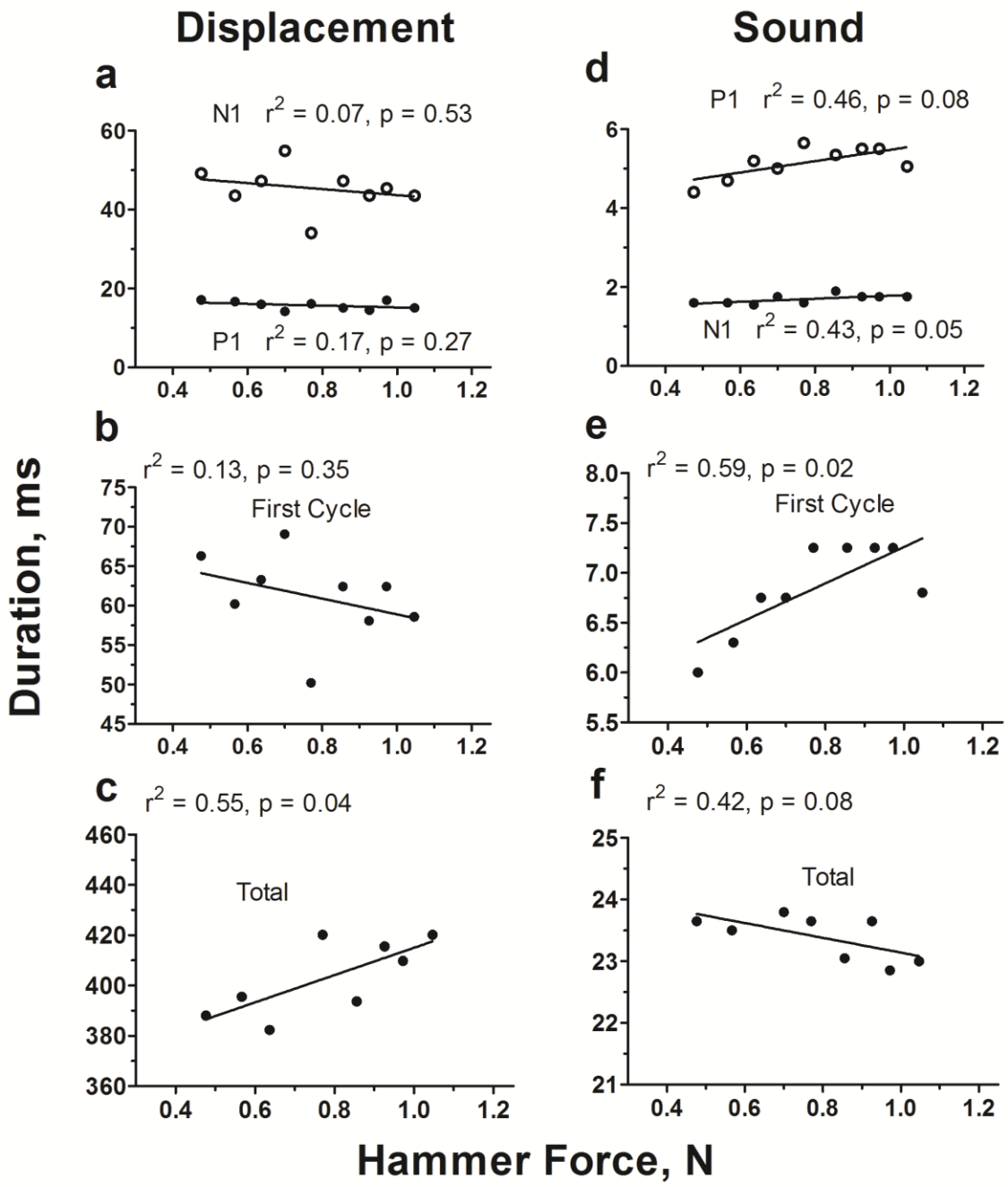

Figure 17: Relationship of displacement and sound (N1, P1, First Cycle, Total) duration to hammer force for the posterior chamber of a carp representative of 8 fish.

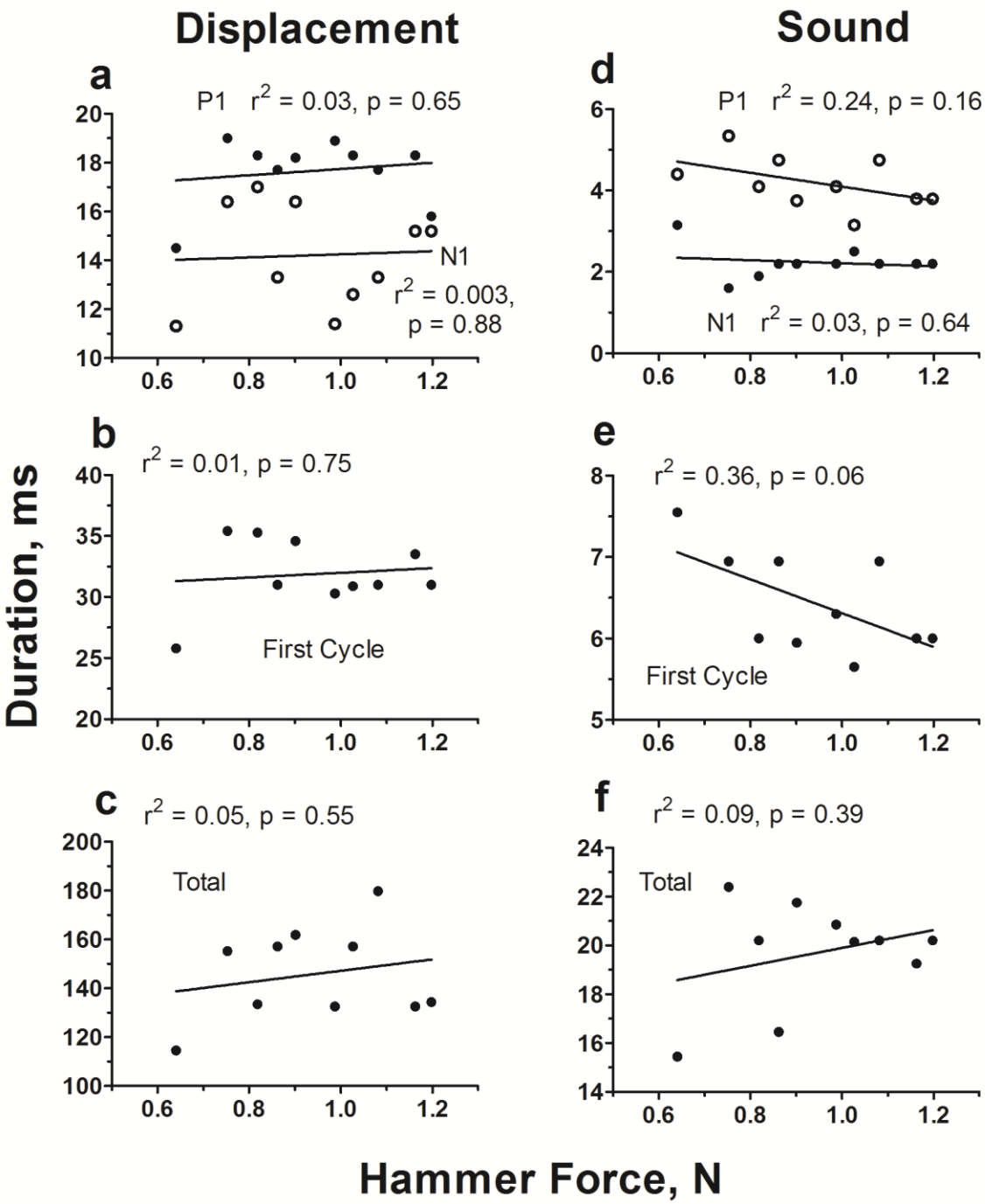

Figure 18: Relationship of displacement and sound (N1, P1, First Cycle, Total) duration for anterior strikes measured for the posterior chamber (AP).

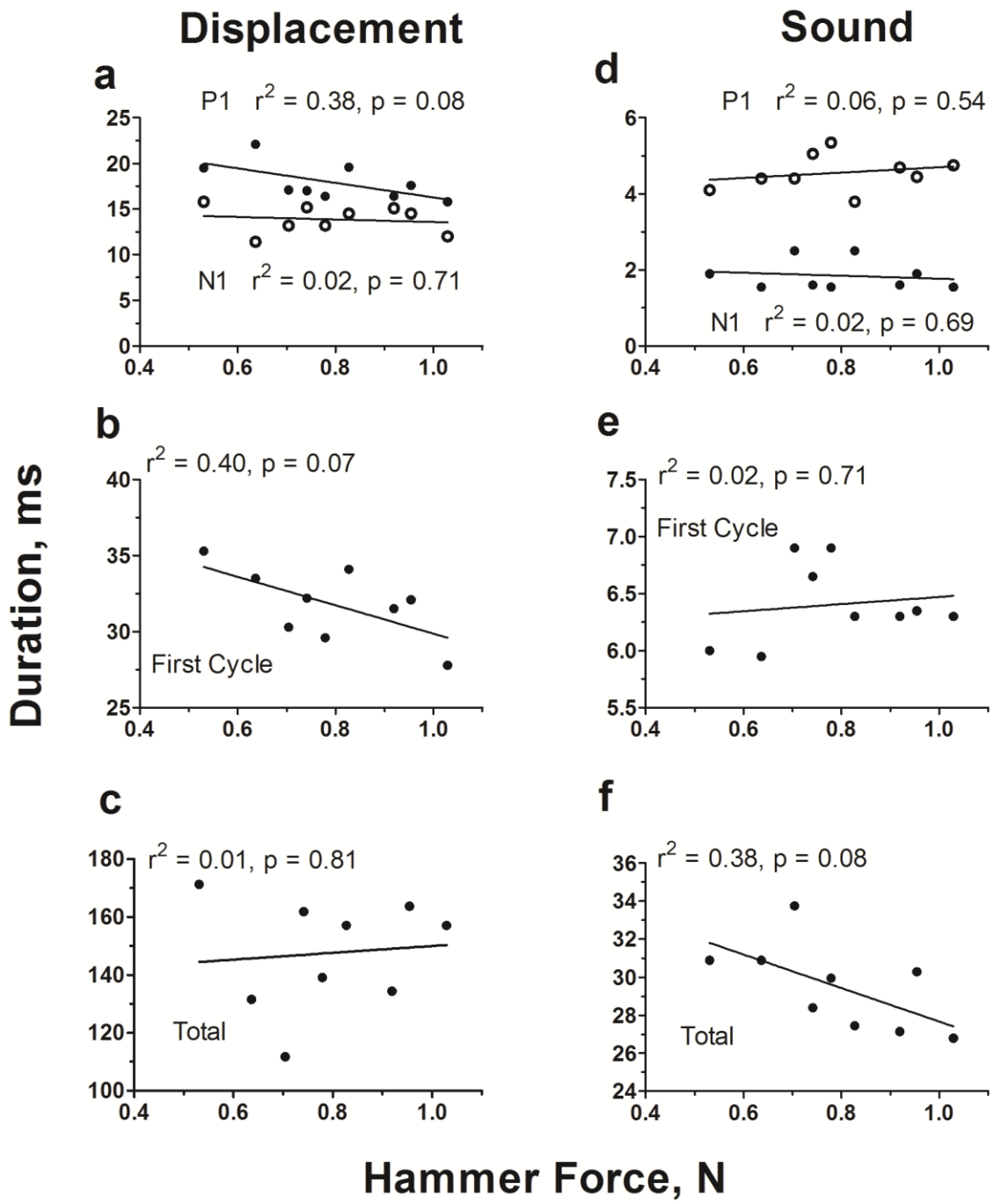

Figure 19: Relationship of displacement and sound (N1, P1, First Cycle, Total) duration for posterior strikes measured for the anterior chamber (PA).

Figure 20: Mean of displacement and sound duration for A, P, AP, and PA. Displacement duration of P1 ($F_{3,28}$ =0.529, p = 0.666) (a), N1 ($F_{3,28}$ = 2.304, p = 0.0986) (b), First Cycle ($F_{3,28}$ = 2.392, p = 0.0897) (c), Total ($F_{3,28}$ = 5.346, p = 0.0049) (d) and sound duration of N1($F_{3,25}$ = 3.456, p = 0.315) (e), P1 ($F_{3,25}$ = 0.5704, p = 0.6397) (f), First Cycle ($F_{3,25}$ = 1.408, p = 0.2639) (g) and Total ($F_{3,25}$ = 0.2359, p = 0.8705) (h).

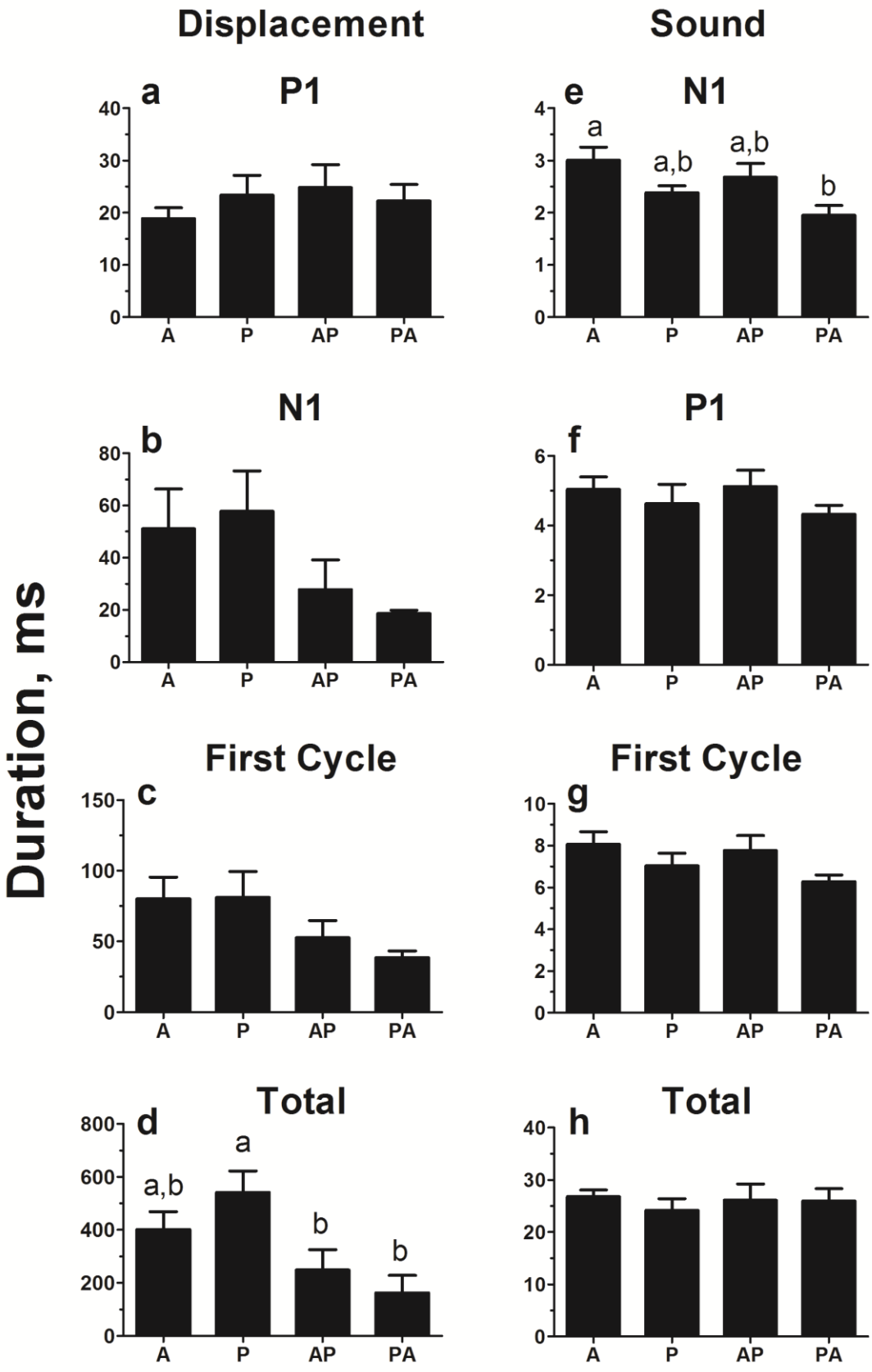
Displacement
Sound
a
P1
e
N1
b
N1
f
P1
c
First Cycle
g
First Cycle
d
Total
h
Total
Duration, ms
A
P
AP
PA
a
a,b
b

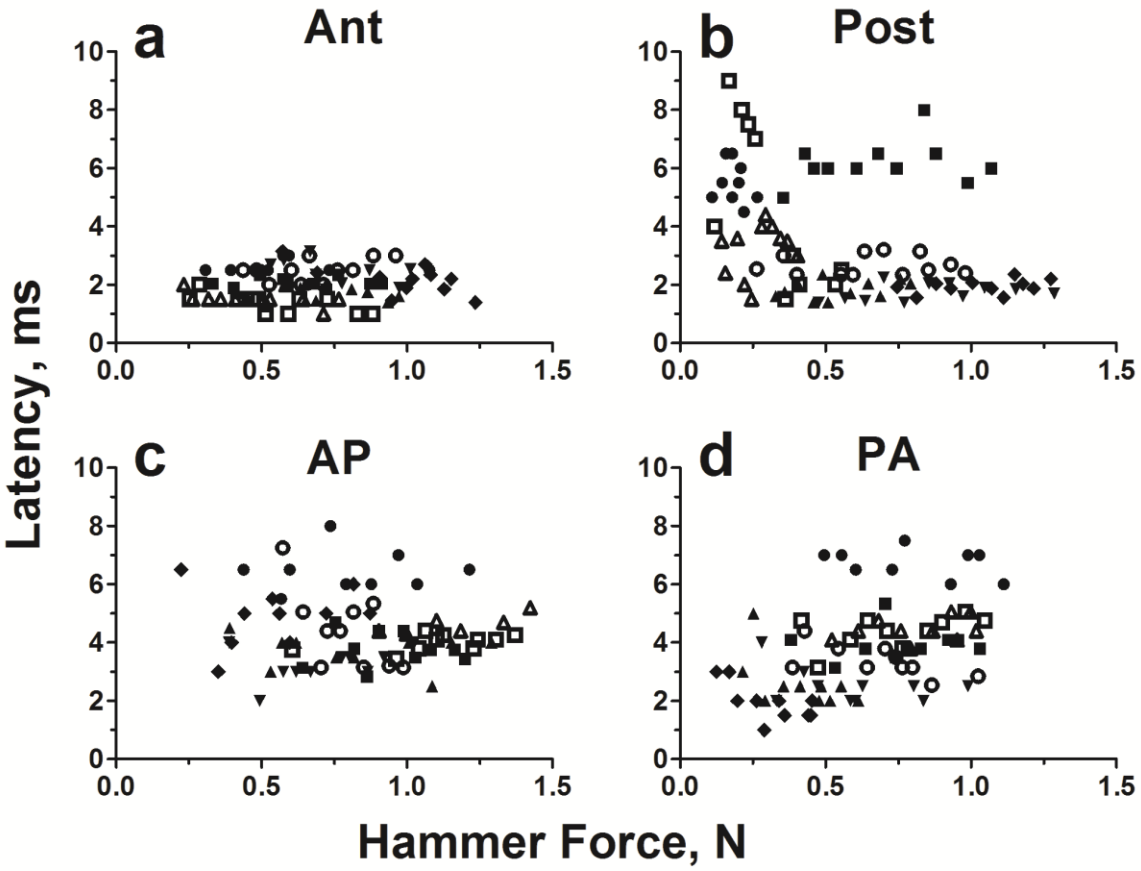

Figure 21: Relationship between hammer force and displacement latency for anterior (a) and posterior (b) chambers and across anterior to posterior (c) and posterior to anterior chambers (d)

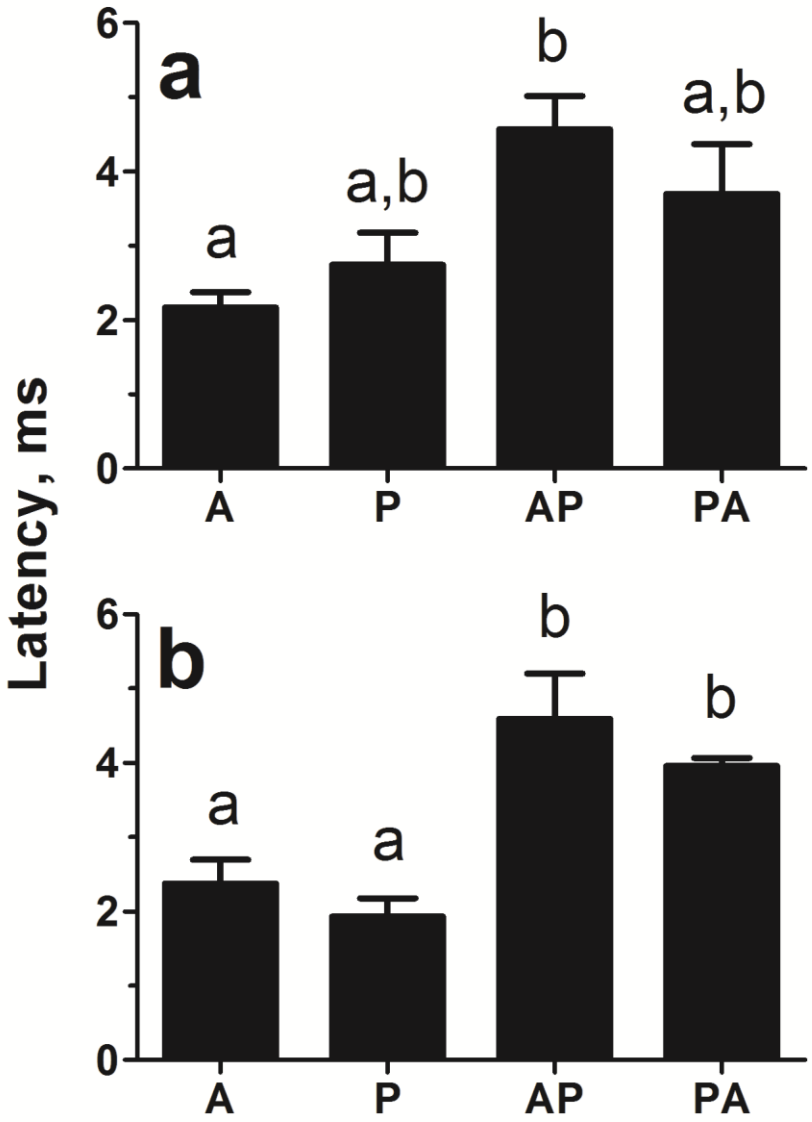

Figure 22: Latency of swimbladder displacement within anterior (A) ($F_{3,27}$ = 5.166, p = 0.006) and posterior (P) ($F_{3,12}$ = 11.70, p = 0.0007) chambers and across anterior to posterior (AP) and posterior to anterior chambers (PA) for all fish (a) and for large fish (b). For all fish and large fish A = 2.1 ± 0.2, 2.4 ± 0.3, P = 2.7 ± 0.4, 1.9 ± 0.2, AP = 4.6 ± 0.4, 4.6 ± 0.6 and PA = 3.7 ± 0.7, 4.0 ± 0.1.

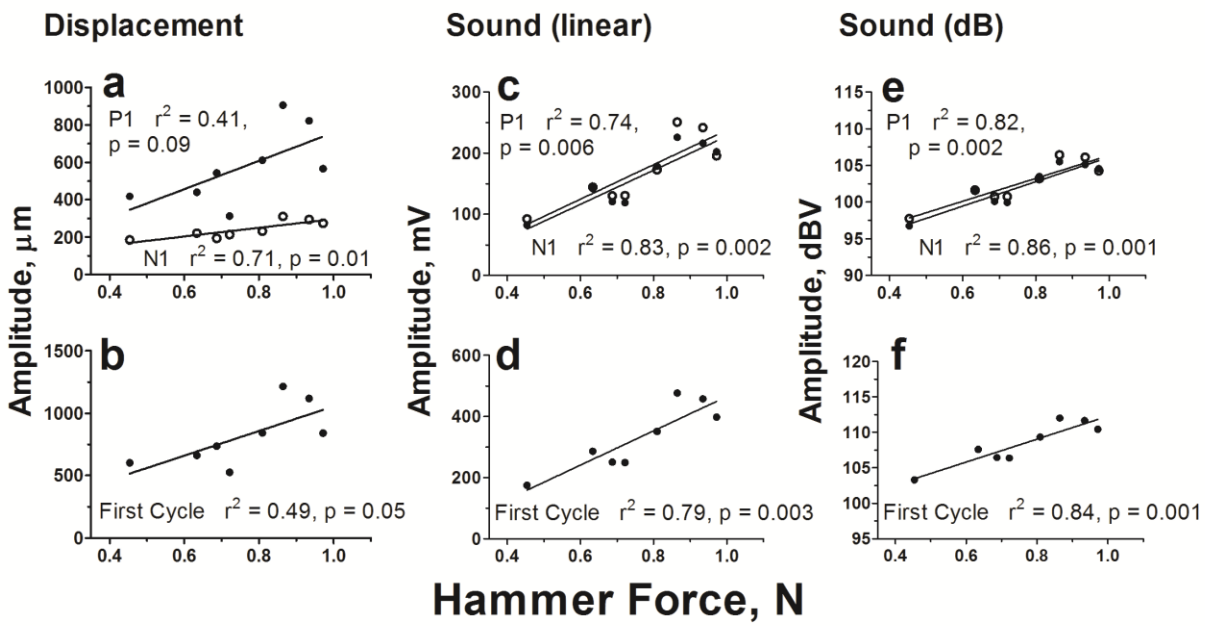

Figure 23: Relationship of displacement and sound (N1, P1, and First Cycle) amplitude to hammer force for the anterior chamber of a carp representative of 8 fish.

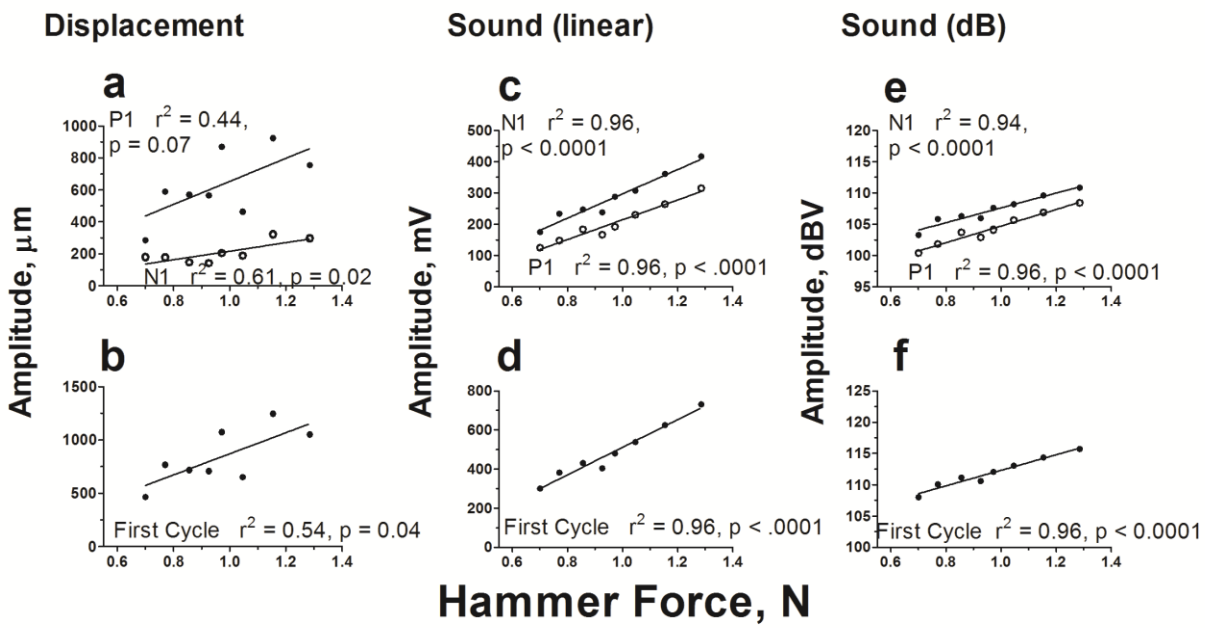

Figure 24: Relationship of displacement and sound (N1, P1, and First Cycle) amplitude to hammer force against posterior chamber for a carp representative of 8 fish.

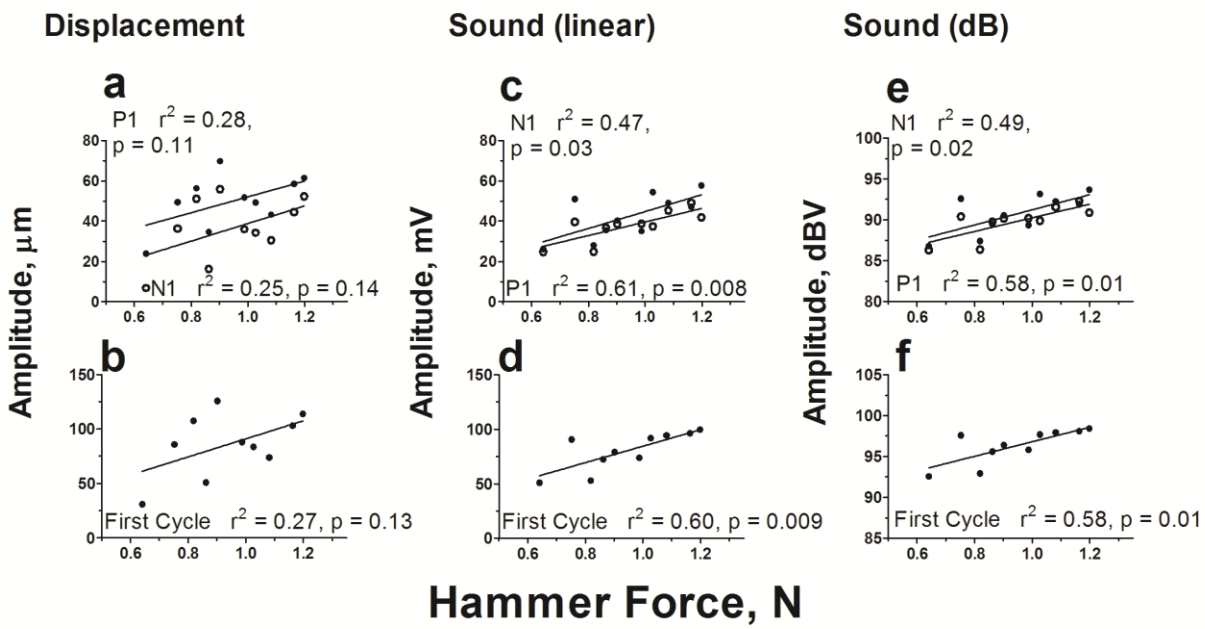

Figure 25: Relationship of displacement and sound (N1, P1, and First Cycle) amplitude for anterior strikes measured for the posterior chamber (AP).

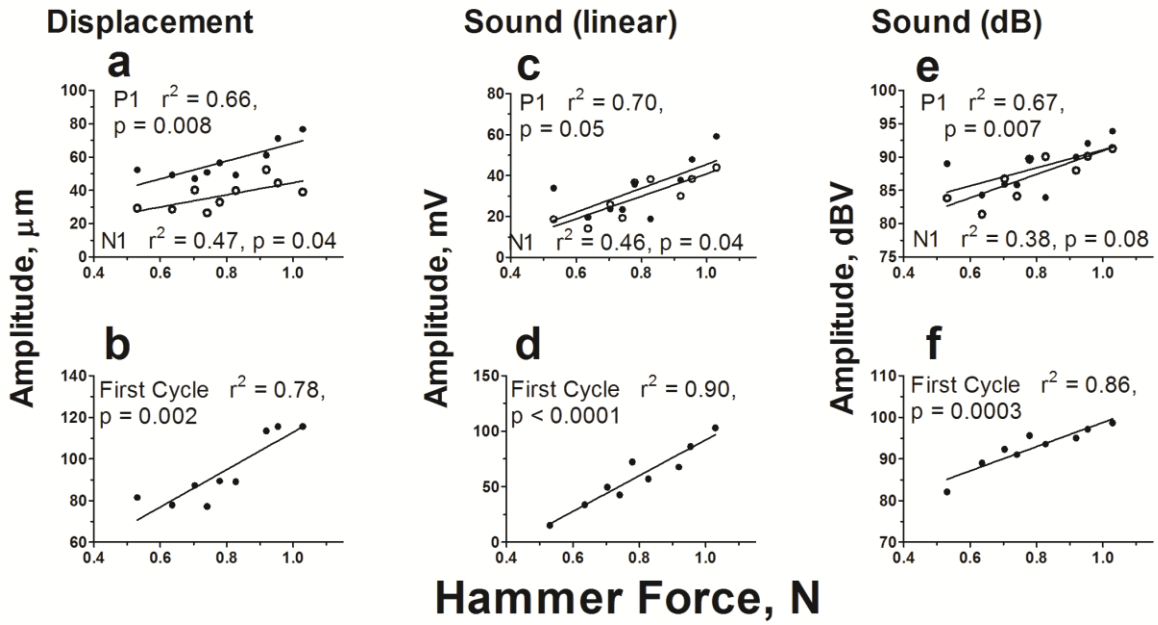

Figure 26: Relationship of displacement and sound (N1, P1, and First Cycle) amplitude for posterior strikes measured for the anterior chamber (PA).

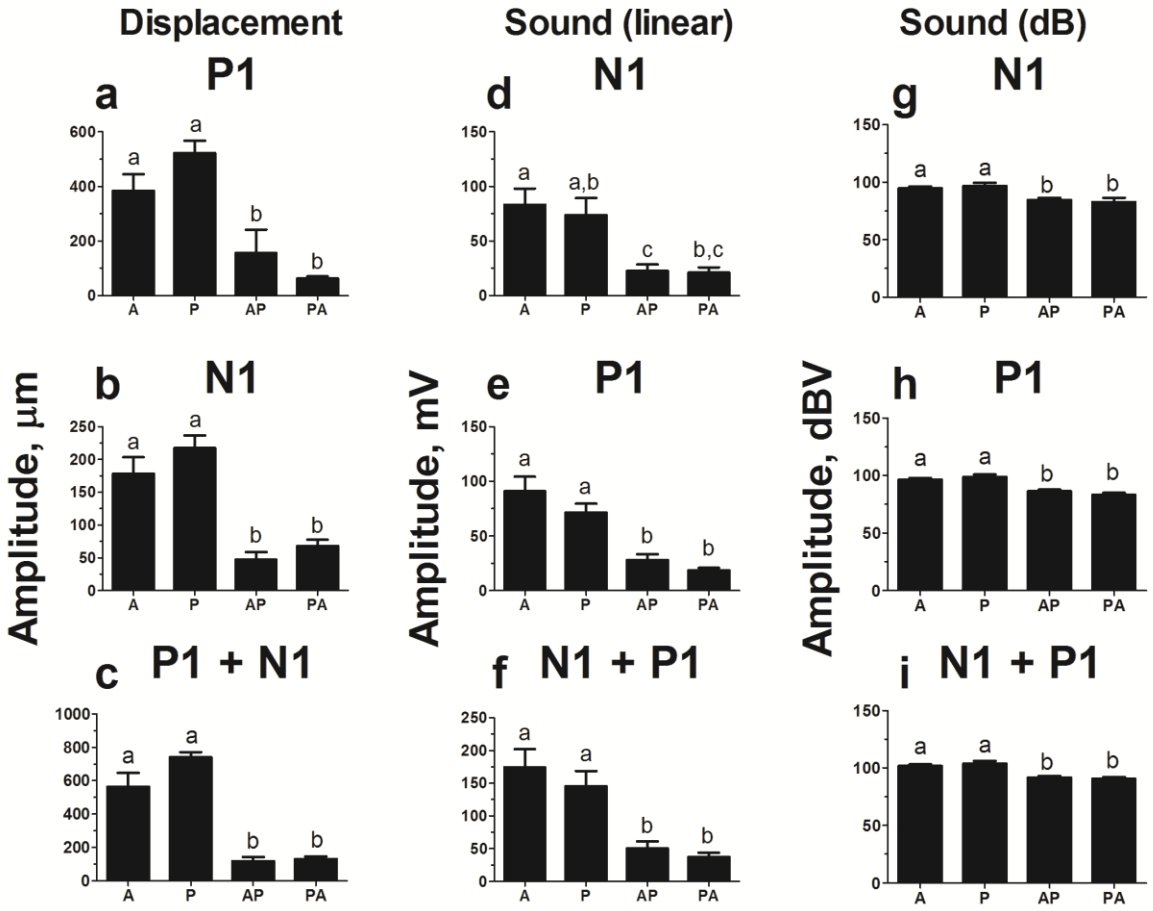

Figure 27: Adjusted mean calculated for 0.63 N strike of displacement and sound amplitude for A, P, AP, and PA. Different letters indicate significantly different means. Displacement amplitude for P1 ($F_{3,24} = 11.01$, $p < 0.0001$) (a), N1 ($F_{3,23} = 22.44$, $p < 0.0001$) (b) and First Cycle (P1+N1) ($F_{3,23} = 40.32$, $p < 0.0001$) (c). Sound amplitude for N1 ($F_{3,25} = 6.878$, $p = 0.0016$) (d), P1 ($F_{3,25} = 13.71$, $p < 0.0001$) (e) and First Cycle (N1 + P1) ($F_{3,25} = 10.1$, $p = 0.0002$) (f). Sound amplitude dBV for N1 ($F_{3,25} = 9.891$, $p = 0.0002$) (g), P1 ($F_{3,25} = 18.6$, $p < 0.0001$) (h) and First Cycle (N1 + P1) ($F_{3,25} = 15.27$, $p < 0.0001$) (i).

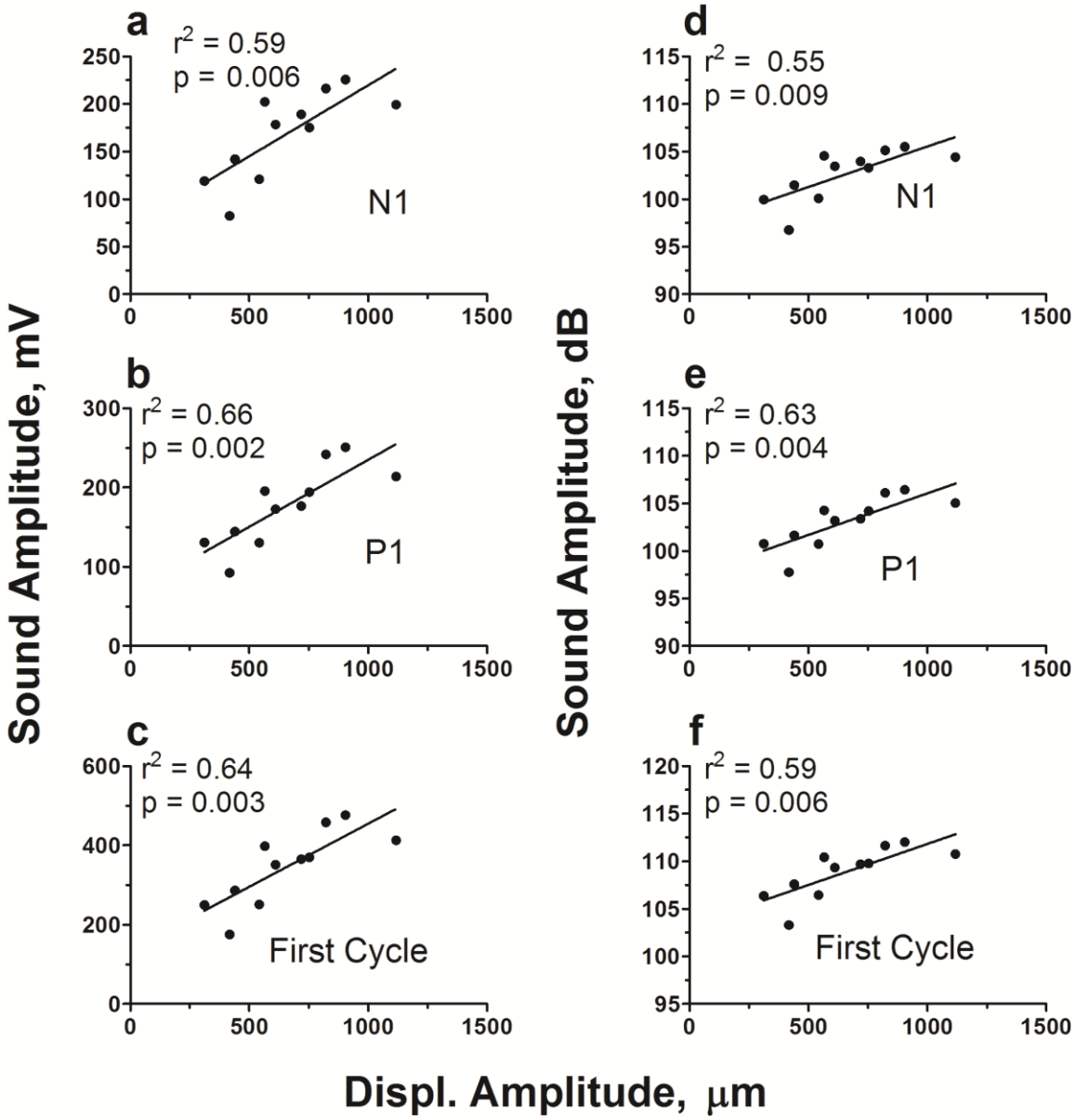

Figure 28: Relationship of evoked sound (N1, P1, and First Cycle) amplitude to P1 displacement for A of a carp representative of 8 fish.

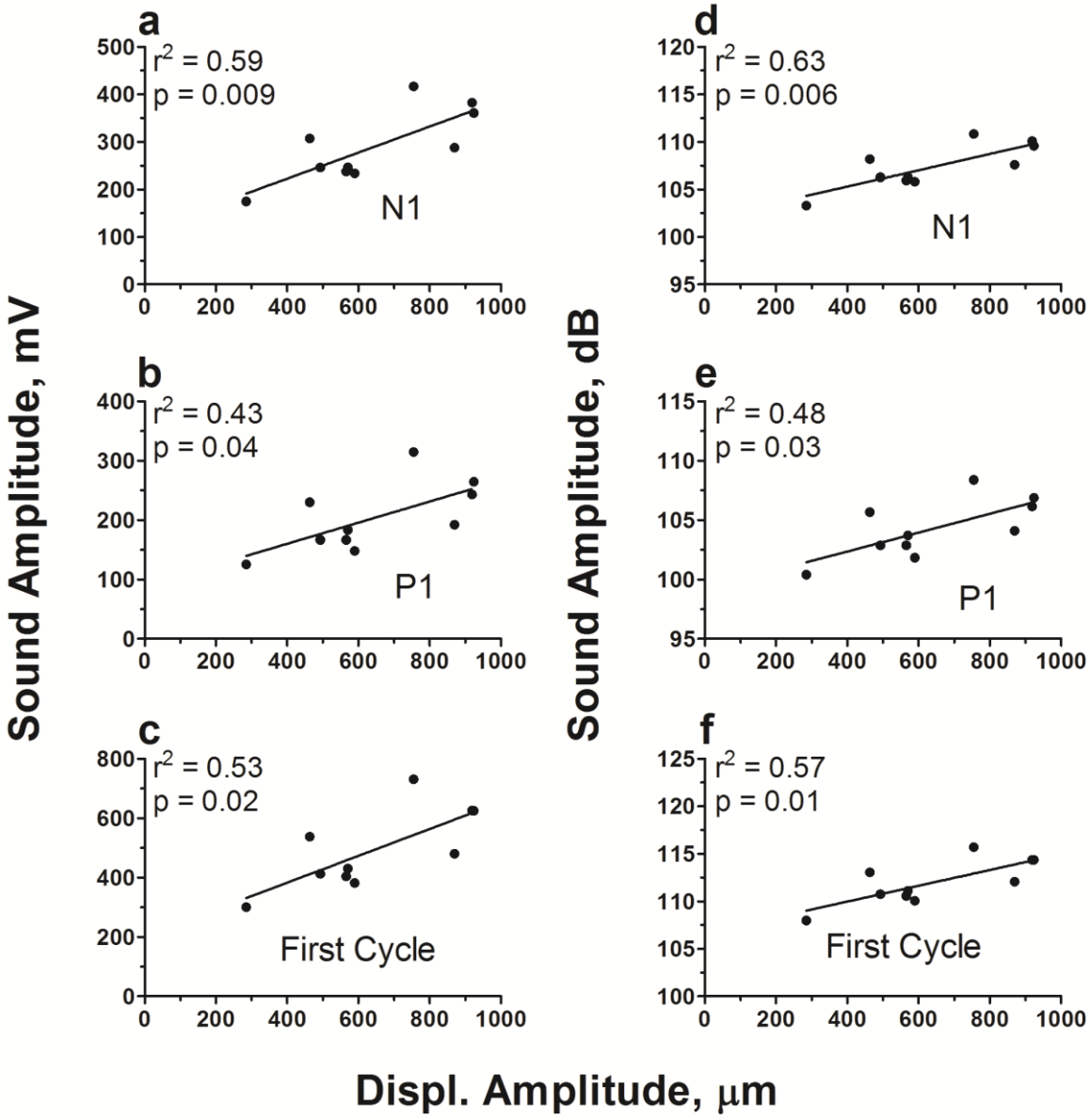

Figure 29: Relationship of evoked sound (N1, P1, and First Cycle) amplitude to P1 displacement for P of a carp representative of 8 fish.

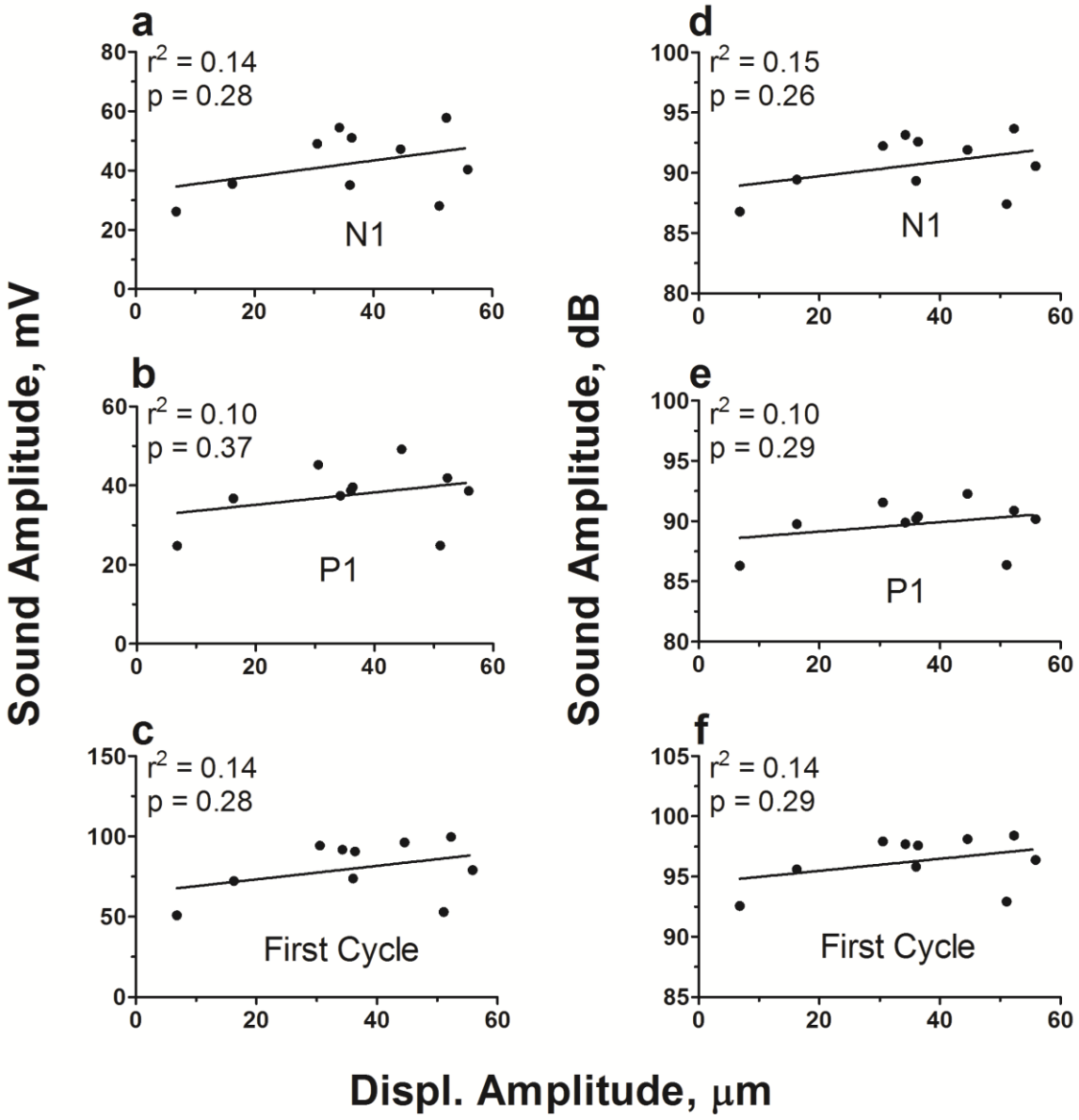

Figure 30: Relationship of evoked sound (N1, P1, and First Cycle) amplitude to P1 displacement for AP of a carp representative of 8 fish.

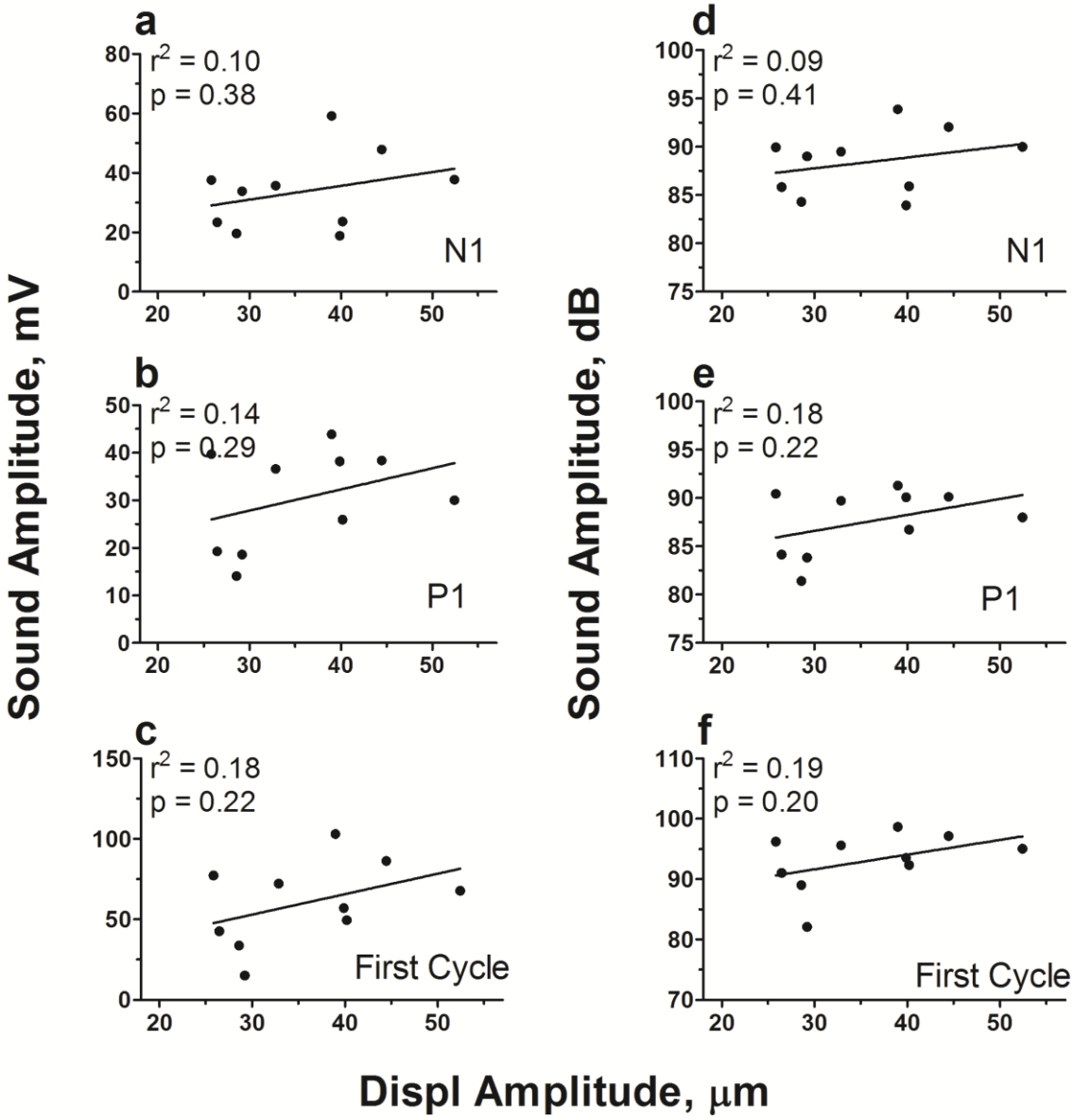

Figure 31: Relationship of evoked sound (N1, P1, and First Cycle) amplitude to P1 displacement for PA of a carp representative of 8 fish.

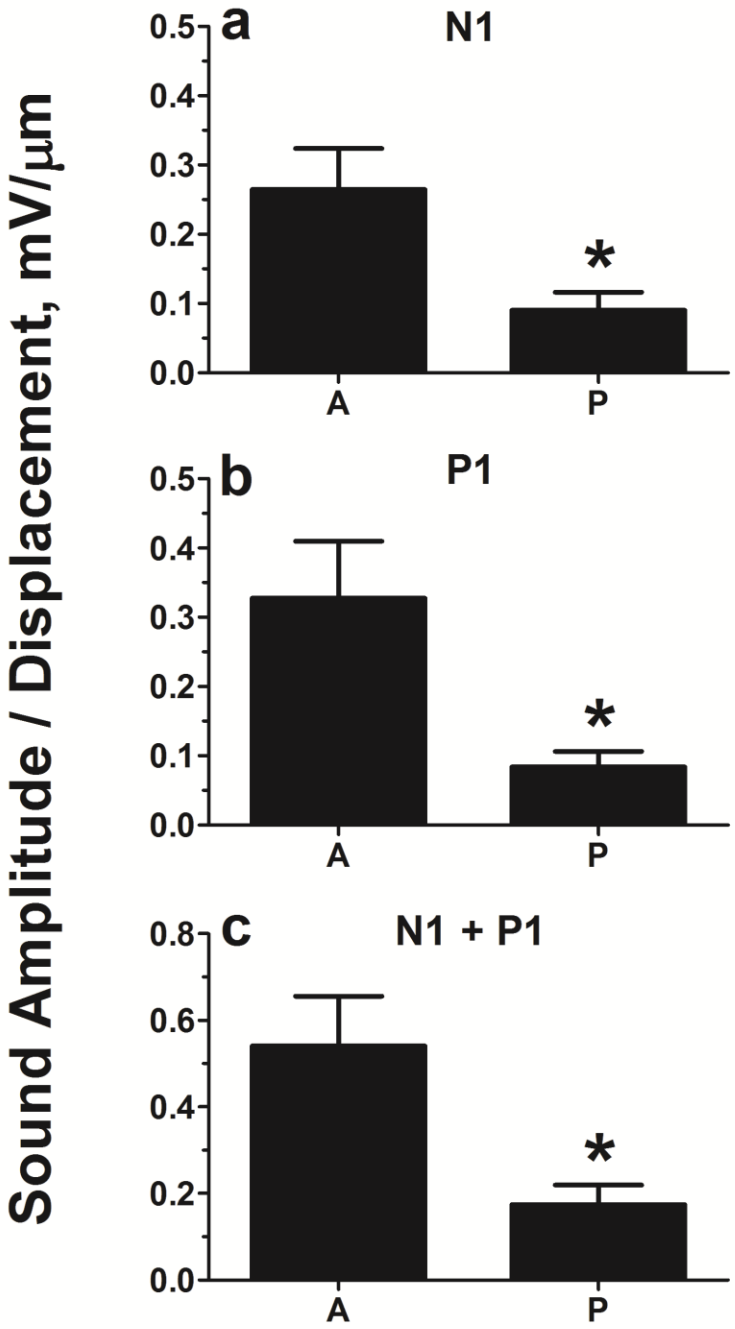

Figure 32: Sound amplitude (mV) per μm of displacement for anterior and posterior chambers of N1 (T_9 = 2.499, p = 0.0339) (a), P1(T_9 = 2.602, p = 0.0286) (b), and first cycle (T_9 = 2.729, p = 0.0232) (c) per millimeter of P1 displacement. For A and P, N1 = 0.26 ± 0.06, 0.09 ± 0.03, P1 = 0.3 ± 0.1, 0.08 ± 0.02 and N1 + P1 = 0.5 ± 0.1, 0.17 ± 0.05.

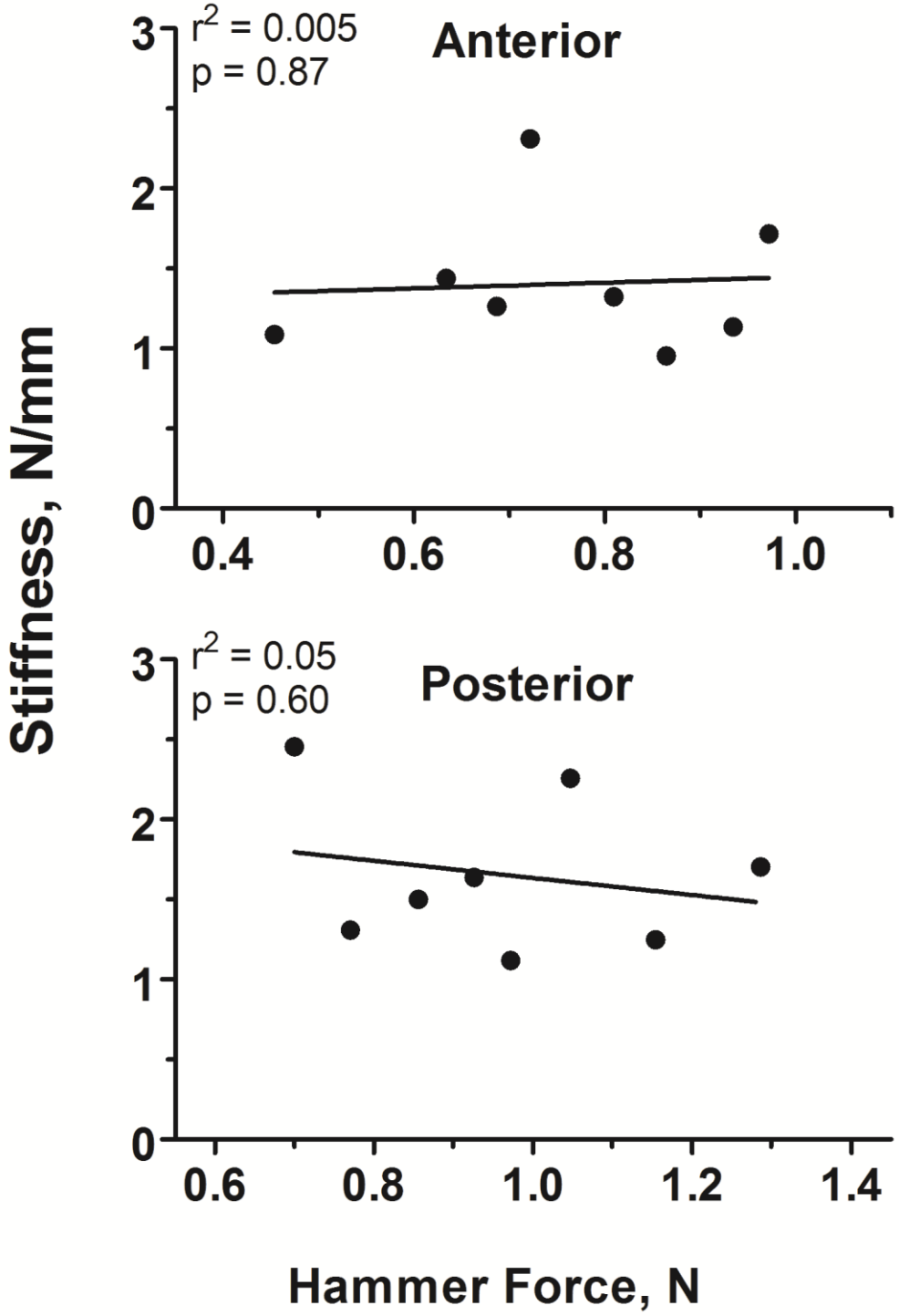

Figure 33: Relationship of stiffness to hammer force against the anterior and posterior chambers for a carp representative of 8 fish.

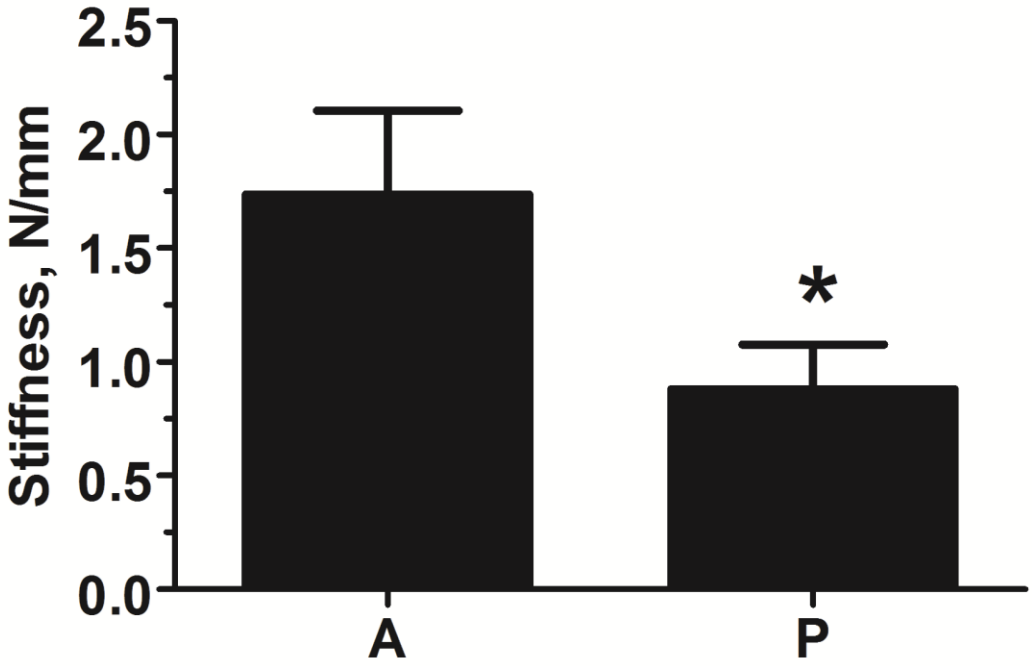

Figure 34: Stiffness, N/mm, for A (1.7 ± 0.4) and P (0.9 ± 0.4) strikes (T_{14} = 2.044, p = 0.0301).

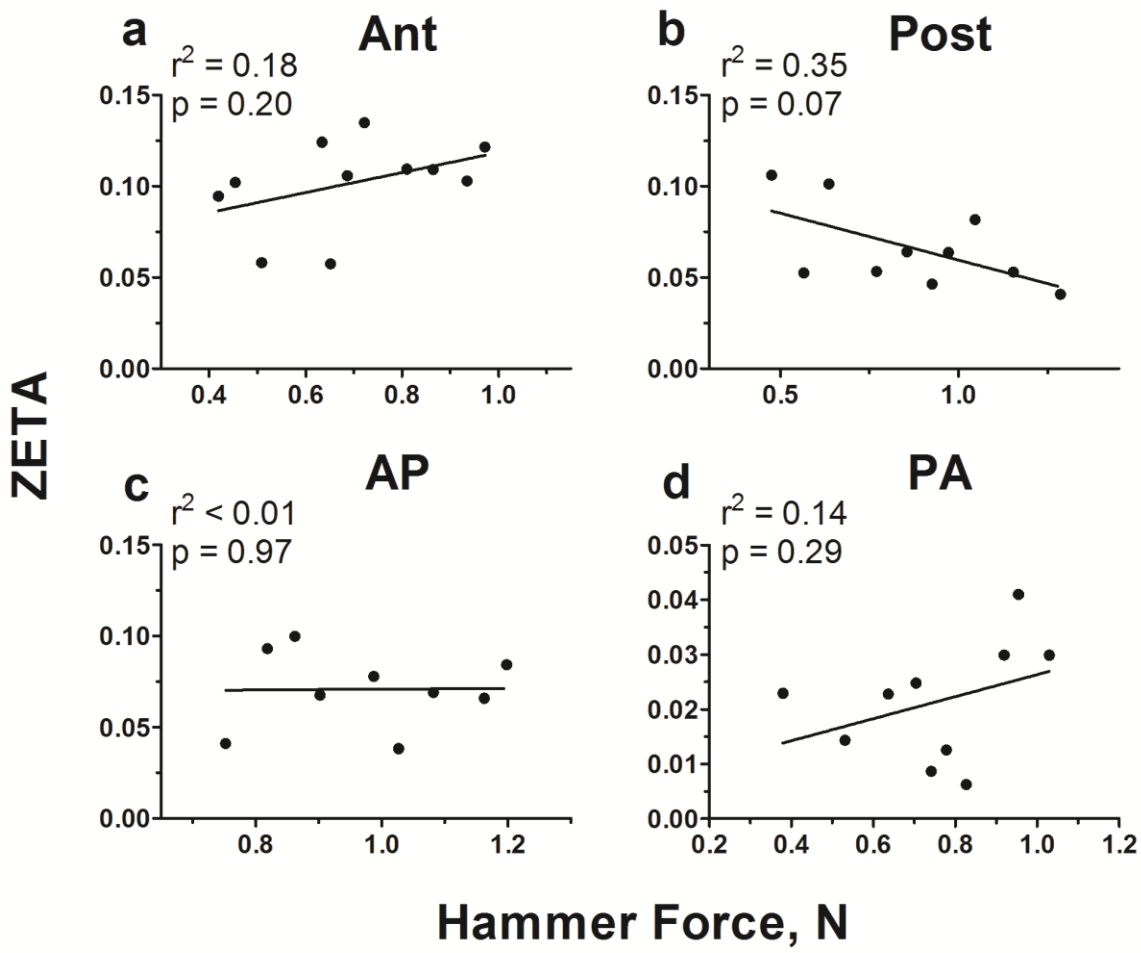

Figure 35: Relationship of damping coefficient, zeta, to hammer force for a carp representative of 8 fish.

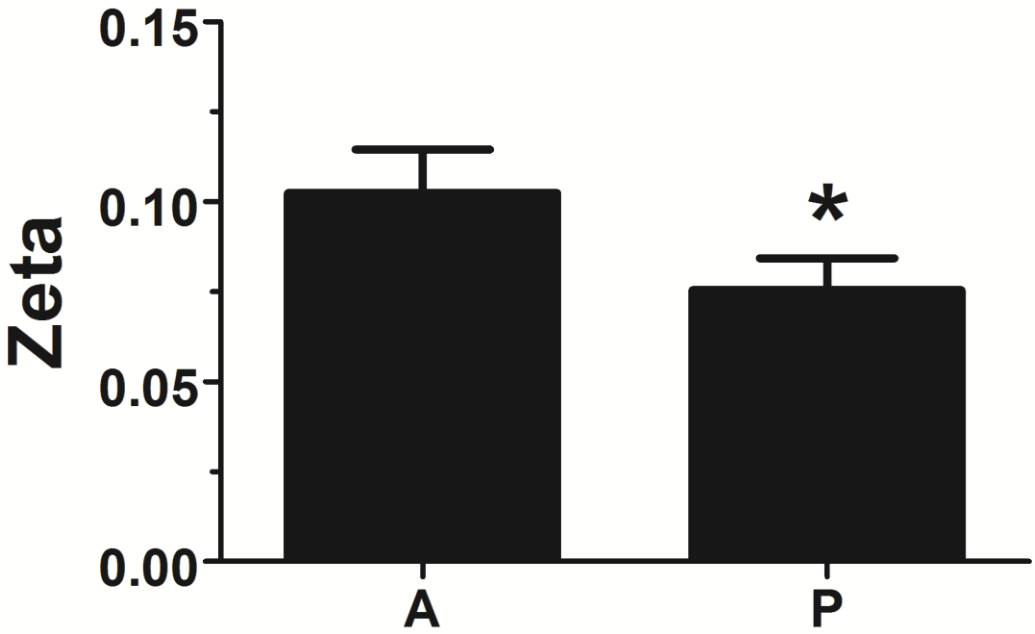

Figure 36: Damping coefficient, zeta, of anterior (0.10 ± 0.01) and posterior (0.075 ± 0.009) chambers (paired $T_7 = 2.549$, $p = 0.0381$)

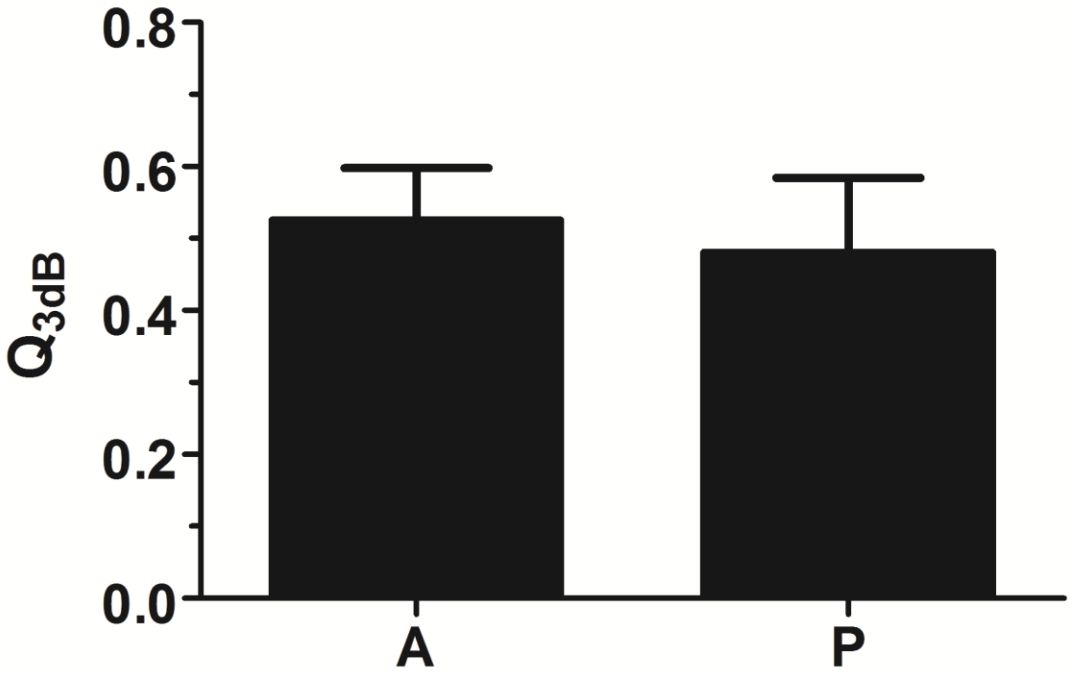

Figure 37: Sharpness of tuning (Q_{3dB}) of evoked sound from anterior (0.52 ± 0.07) and posterior (0.5 ± 0.1) chambers (T_7 = 0.8979, p = 0.3991).

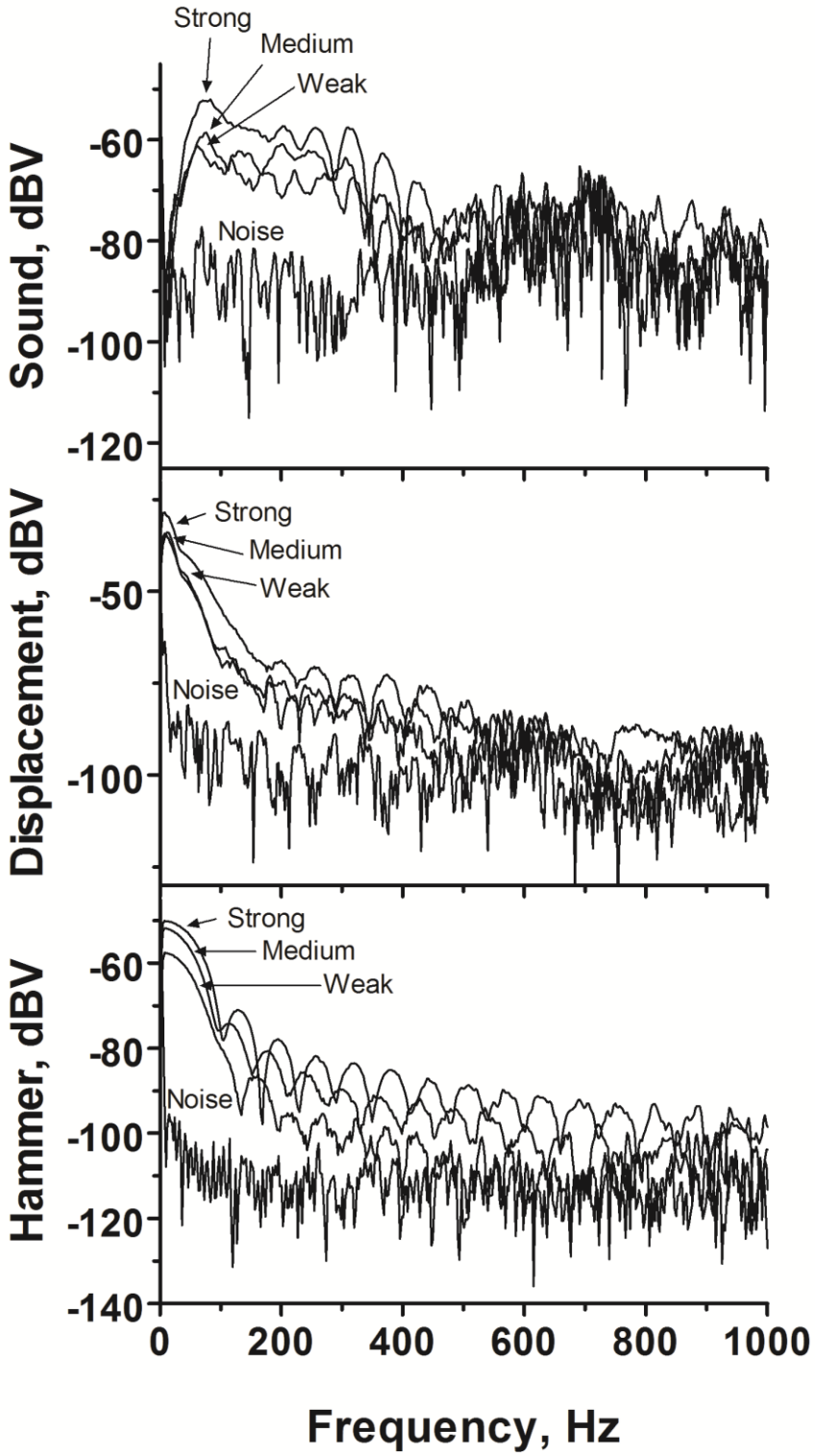

Figure 38: Frequency spectra for the hammer strike and induced swimbladder displacement and sound for a representative carp for weak, medium and hard hammer hits.

Vita

Yasha Joseph Mohajer was born on April 28, 1983 in Terre Haute, Indiana. He graduated from Midlothian High School in Midlothian, Virginia in 2002, received his Bachelor of Science in Biomedical Engineering from Virginia Commonwealth University, and received his Master of Science from Virginia Commonwealth University 2011.